Glucan Particle Delivery of Mesoporous Silica-drug Nanoparticles

A Major Qualifying Project Report

Submitted to the Faculty of the

WORCESTER POLYTECHNIC INSTITUTE

in partial fulfillment of the requirements for the

Degree of Bachelor of Science

in

Chemistry and Biochemistry

by

_____   _____

Abaigeal Caras   Lindsey Kut

April 28, 2011

APPROVED:

_____   _____

Ernesto Soto, Ph.D.   Destin Heilman, Ph.D.
Molecular Medicine   Biochemistry
UMASS Medical School   WPI Project Advisor
Major Advisor

Table of Contents

Abstract

Glucan particles (GPs) are 2-4 um hollow, porous shells extracted from Baker's yeast, *Saccharomyces cerevisae.* The GP surface is composed primarily of 1,3-B-glucan allowing for efficient receptor-mediated particle uptake by phagocytic cells expressing glucan receptors. GPs have been used for macrophage-targeted delivery of payload macromolecules (i.e. DNA, siRNA, protein). Mesoporous silica nanoparticles (MSNs) are materials synthesized from tetraorthosilicate reacting on a template to produce particles with a regular arrangement of pores. The large surface area of the MSN pores allows for efficient drug encapsulation. In this project, a model combined GP/MSN drug delivery system was developed using the chemotherapeutic drug doxorubicin (Dox) and the antibiotic rifampicin (Rif). The GP/MSN system benefits from the macrophage targeting capabilities of GPs and small drug molecule binding capacity of MSNs. GP/MSN samples containing Rif were studied for their effect on inhibiting *E. coli* growth. GP/MSN formulations containing Dox were evaluated for Dox delivery and growth arrest of the model murine cell line NIH3T3-D1.

1. Introduction

This project was developed to establish experimental methods to prepare glucan particles (GPs) containing mesoporous silica nanoparticles (MSNs) for small drug molecule targeted delivery to macrophages. It is the goal of this project to synthesize GPs containing MSNs to create a delivery agent that benefits from the macrophage targeting capabilities of glucan particles and small drug molecule binding capacity of MSNs.

1.1 Glucan particle delivery technology

Delivery agents play crucial roles in the synthetic transportation of materials into cells. An effective delivery agent is defined by three key characteristics. First, the delivery agent must protect the material being transported and preserve the material from degradation. Second, the material needs to be successfully delivered into the target cells through the cell membrane. The last characteristic is that the delivery agent should have minimal detrimental effects on the target cell (Soto & Ostroff, Characterization of Multilayered Nanoparticles Encapsulated in Yeast Cell Wall Particles for DNA Delivery, 2008).

In order to create empty shells that can be used for transportation, Baker's yeast (*Saccharomyces cerevisiae*) is processed by chemical extractions into particles of different carbohydrate and lipid compositions. Baker's yeast particles can be synthesized into delivery agents that are characterized as being hollow, biodegradable, porous particles that range from 2 – 4 µm in diameter (Figure 1). The primary carbohydrate composition of a Baker's yeast particle is β-1, 3-D-glucan (~85%), glycogen, water and

ash, with <1% residual levels of chitosan/chitin, and mannoproteins (Young, et al., 2007).

The high β-1, 3-D-glucan composition of the particle surface allows for efficient

phagocytosis via receptor-mediated cell uptake by cells expressing glucan receptors

(dectin-1 (D1) and complement receptor 3 (CR3 or CD11b/CD18)), such as monocytes,

macrophages, neutrophils and dendritic cells (Brown & Gordon, 2001) . GP uptake has

been demonstrated to be dectin-1 dependent *in vitro* as shown in Figure 2. Bone marrow

dendritic cells (BMDC), from a wild type mouse, efficiently phagocytize fluorescently

labeled GPs. BMDCs from a dectin-1 knockout mouse do not show GP uptake.

Furthermore the addition of a laminarin, a soluble β -glucan, inhibits GP uptake in the

wild type BMDCs. (Huang, Ostroff, Lee, Wang, Specht, & Levitz, 2009).

Depending on the chemical extraction treatment (acid/base, organic solvent

extraction) it is possible to obtain GPs of slightly different chemical compositions. Three

examples of particles derived from Baker's yeast include standard glucan particles (GPs),

glucan mannan particles (GMPs), and glucan lipid particles (GLPs). Standard GPs are

composed primarily of β-1, 3-D-glucan and low levels of chitin. GPs have gone through

the highest level of purification in comparison to the GMPs which still consists of β-1, 3-

D-glucan, mannoproteins, and chitin (Soto & Ostroff, Characterization of Multilayered

Nanoparticles Inside Yeast Cell Wall Particles for DNA Delivery, 2008). The last

variation of Baker's yeast particles is the GLPs. GLPs also have β-1, 3-D-glucan and a

low level of chitin, like the GP, but the GLP also has a lipid layer remaining. The lipid

layer is predominantly composed of sterols (squalene, zymosterol, ergosterol and

lanosterol) (Sajbidor & Gergoa, 1994). This lipid layer allows for better loading of

hydrophobic compounds than the standard GPs

Glucan particles are an alternative non-viral macromolecular delivery vehicle. Macromolecules (i.e. DNA, siRNA, proteins, vaccines) can be trapped inside the hollow particle cavity by electrostatic interactions between the payload molecules and trapping polymers forming polyplexes. Depending on the location of the payload drug there are three possible GP-polyplex formulations as shown in Figure 3. The advantages of the glucan particle delivery system include, high binding capacity, as well as the co-encapsulation of a wide variety of possible guest molecules in the polyplex structures with specific functions to facilitate payload release upon uptake of the GPs by target cells (Soto & Ostroff, Characterization of Multilayered Nanoparticles Inside Yeast Cell Wall Particles for DNA Delivery, 2008) (Aouadi, et al., 2009) (Soto & Ostroff, Oral Macrophage Mediated Gene Delivery System, 2007) (Tesz, et al., 2011).

Glucan particles have also been used for the delivery of small drug molecules. However, since the majority of small drug molecules are neutral, monovalent in charge, or insoluble in water, such payloads are not effectively trapped within glucan particles using core or LbL encapsulation methods. Previous studies have shown the use of glucan particles for the delivery of small molecules using hydrogels to physically entrap the drug (i.e. rifampicin) inside the particles instead. These studies showed effective reduction *in vitro* of intracellular Tuberculosis levels in infected bone marrow derived macrophages with GP-Rif formulations at sub-MIC (minimum inhibitory concentration) levels of the antibiotic. However, the formulations were not effective for controlled drug release limiting its *in vivo* application (Soto E. , Kim, Lee, Kornfield, & Ostroff, 2010).

Recent advances in glucan particle delivery technology include the ability to encapsulate pre-formed nanoparticles (NPs) of less than 30 nm in diameter into GPs and to non-covalently bind larger nanoparticles to the outer surface of a derivatized glucan particle (Figure 4). Nanoparticles of less than 30 nm (i.e. fluorescently labeled 20 nm polystyrene, 10 nm magnetic iron oxide NPs, and 10 nm quantum dot nanoparticles) have been efficiently trapped inside GPs. The advantages of nanoparticle encapsulation are: (1) it extends the applicability of the glucan particle delivery system by allowing encapsulation of materials that cannot be prepared *in situ* as the synthetic conditions are not compatible with glucan particles, (2) this allows for incorporation of nanoparticles that can enhance the ability to load small drug molecules (neutral, hydrophobic drugs) into GPs, and (3) it allows for incorporation of nanoparticles with an intrinsic property, such as magnetic nanoparticles, thus increasing the versatility of the particles, as the same formulation could be used for drug delivery and the magnetic properties employed for cell purification, or imaging applications (Soto & Ostroff, 2011) (Soto & Ostroff, Use of beta-Glucans for Drug Delivery Applications, 2011) (Soto & Ostroff, Encapsulation of Nanoparticles Inside Yeast Cell Wall Particles for Receptor-targeted Drug Delivery, 2010).

1.2 Mesoporous Silica Nanoparticles

Mesoporous silica nanoparticles (MSNs) were first developed in the labs of the Mobil Corporation in 1992 and originally named Mobil Crystalline Materials or MCM-41 (Kresge, Leonowicz, Roth, Vartuli, & Beck, 1992). MSN was developed as an inorganic delivery agent. These nanoparticles are of interest because of their high

chemical and thermal stability. MSNs are synthesized by reaction of tetraethyl orthosilicate (TEOS) and a template, which form nano-sized spheres or rods (Figures 5-6). The basic structure of a MSN is of a particle 50-500 nm in diameter with pores ranging from 2 to 20 nm in size. These pores are mostly cylindrical in shape (Kresge, Leonowicz, Roth, Vartuli, & Beck, 1992) but range in the level of order of their molecular organization. The basic structure of these molecules lends themselves to be used for absorption, catalysis, chemical expression, or for use in chemical devices (Trewyn, Slowing, Giri, Chen, & Lin, 2007). Through the process of different syntheses it is possible to control the morphology and porosity of these small cylindrical particles. Furthermore, MSN can be functionalized externally and internally with organic and inorganic groups due to its large internal and external surface areas.

Since the discovery of MSN in 1992, scientists have been working to gain more control over its' specific characteristics. More recent work has been focused on the controlled release and delivery of drugs. Chemical modification of MSN allows incorporation of functional groups to facilitate absorption of target compounds (i.e. cationic MSNs for binding of nucleic acids). Modification of the external surface of the MSN has been done to introduce targeting ligands. In these ways, MSNs can be modified to be taken up by a specific receptor mediated process by target cells to complete controlled release of genes and drugs within the cell. Limitations exist in this because the introduction of ligands to the nanoparticles is synthetically challenging and the MSNs are produced at a high expense with a low yield.

1.2.1 Mesoporous Silica Nanoparticle Synthesis

The basic synthesis of MSNs can be performed in acidic or basic conditions. The process begins with the surfactant, cetyltrimethylammonium bromide (CTAB), dissolved in water. Tetraethylorthosilicate (TEOS) is then added to this solution and heated for several hours. Following complete polymerization of the TEOS reagent, the CTAB is then extracted from the solution through reflux. By manipulating temperature, micelle formation, co-solvent and pH during this process, the size and shape of the nanoparticles that are generated can be controlled. It is important to complete the reaction at a low surfactant concentration to make the assembly of the MSN dependent upon the interactions between the cationic surfactant and the growing anionic oligomers of orthosilicic acid. This, in turn, will limit the MSN to a small size (Trewyn, Slowing, Giri, Chen, & Lin, 2007). The synthetic scheme of MSN using TEOS is depicted in Figure 5.

Within a MSN there are two distinct surfaces including the external and internal surfaces, both of these surfaces can be further functionalized with active groups. There are two processes to functionalize the surfaces of MSN; the first process is called grafting. Grafting can be completed with post-synthesis nanoparticles to selectively functionalizing the exterior surface of the MSN. The organosilanes, organotrialkoxysilanes or organotrichlorosilanes, are reacted with the MSN in a non-polar anhydrous solvent. This method usually leads to most of the organosilanes binding to the exterior of the MSN or in the openings of the pores (Trewyn, Slowing, Giri, Chen, & Lin, 2007).

The second method for functionalizing the MSN is called the co-condensation method. In this direct synthesis method, a co-condensing agent is added to the aqueous CTAB and TEOS solution during condensation to control the shape of the MSN. The co-condensing agent will allow for control of the morphology of the particles along with the type and degree of functionality. The characteristics of the co-condensing agent that should be considered include concentration, molecular size, and hydrophobicity or hydrophilicity. These properties will determine the ability of the co-condenser to influence the stabilization of the micelles during the formation of MSN.

The formation of individual cylindrical micelles is stabilized by non-polar groups interacting with hydrocarbon tails of the surfactant templates. As a result, the charge density of the head group is reduced. This group exhibits "side on" growth of the silicate coated cylindrical micelles, generating rod shaped nanoparticles. Both variations of MSN can be seen in Figure 6. On the other hand, when the co-condensing agent is more hydrophilic there is no further stabilization; therefore little "side on" condensation growth is seen. In this scenario, formation of long micelles is rendered. Small spherical particles, that resemble the molecules that were achieved with no co-condensation agent, are created instead (Trewyn, Slowing, Giri, Chen, & Lin, 2007).

Using the co-condensing method, it is possible to obtain monodisperse, multi-functionalized MSN. The MSN can have the ability to tune the relative ratios of the functional group of interest. In this process two different co-condensing agents are used that have diverse structure directing abilities. This allows the synthesis of particles with

specific pore and particle morphologies. By changing the ratios of the two organic

functional groups used as co-condensing agents, one is able to control the shape and size.

Also, it is possible to control functionality by changing concentrations of co-

condensing agents; not only can the type of functionality be altered but also the degree

(Trewyn, Slowing, Giri, Chen, & Lin, 2007). Specifically, the surface of MSN has been

modified to cap the pores to prevent rapid release, incorporation of magnetic

nanoparticles for cell purification, or targeting ligands for a receptor mediated cell

uptake.

1.2.2 Mesoporous Silica Nanoparticles for Cancer Therapy

For the most part, anticancer therapeutic drugs are hydrophobic in nature and

therefore present challenges for optimal targeted delivery. Mesoporous silica

nanoparticles are consequently important in the administration of these drugs to increase

their aqueous solubility. It is highly important to first encapsulate the drug before (Gillies

& Frechet, 2005) dispensation in order to overcome any issues with low solubility (Lu,

Liong, Zink, & Tamanio, 2007).

MSN has the advantage of having low toxicity. Cell uptake of MSN occurs

mainly by an endocytosis process. Receptor targeted phagocytosis has been accomplished

by further modification of the outside surface of MSN with targeting ligands. In order for

the MSN to carry the hydrophobic cancer drugs, the drugs must first be suspended in

DMSO. This allows the drugs to be absorbed by the MSN and the DMSO can then be removed through washing and centrifugation.

The application of MSN to deliver cancer drugs, as mentioned above, has already been successfully demonstrated with MSNs of 130 nm in size with 750 pores that were each about 2 nm in diameter. The particles were loaded with the hydrophobic anticancer drug camptothecin or the drug paclitaxel. Both of these drugs were successfully absorbed by the MSN and delivered to the target cells (Lu, Liong, Sherman, Xia, Kovochich, & Nel, 2007). In the mainstream pharmaceutical world, about 40% of drugs have low solubility in water; advances in MSN could vastly improve the efficiency and application of these drugs (Lu, Liong, Sherman, Xia, Kovochich, & Nel, 2007).

1.3 Synthesis of Mesoporous Silica and Glucan Particles

Individually MSNs and GPs both contain useful drug delivery characteristics, but also have their limitations. MSNs have the ability to absorb both hydrophobic and hydrophilic small drug molecules, but have no cell targeting specificity unless the MSN is chemically modified to introduce targeting ligands. GPs have limitations in the binding of small drug molecules, especially hydrophobic drugs, but provide selective targeted delivery to innate immune cells (macrophage cells) that express glucan receptors. GPs also have a high binding capacity for pre-formed nanoparticles, making them a suitable encapsulation system for mesoporous silica-drug nanoparticles. The synergy of this approach is expected to create a successful delivery agent that benefits from (1) the binding capacity of MSNs and (2) macrophage targeted delivery by GPs. Specifically, in

this project, the drugs Rifampicin (Rif) and Doxorubicin (Dox) were incorporated into MSN-GPs formulations and delivered to macrophage cell lines and primary cells with glucan receptors.

The GPs were combined with MSNs through three different methods (Figure 7). The first method consisted of loading the pre-formed MSNs inside of the GPs; the second method included loading the soluble MSN reagents into the GPs followed by *in situ* synthesis of MSN; the third method included non-covalent binding of anionic or cationic MSNs to the modified surface of the GPs.

1.3.1 Payload Drugs

Mesoporous silica nanoparticles were tested as drug delivery agents using two slightly hydrophilic drugs, Rifampicin (Rif) and Doxorubicin (Dox). The molecular structures of Rif and Dox can be seen in Figures 8 and 9.

Rifampicin and doxorubicin were chosen for this project for specific reasons. Rifampicin is one of the few small drug molecules that has been previously studied with glucan particles (Soto E. R., Kim, Lee, Kornfield, & Ostroff, 2010). Therefore, the GP-MSN-Rif formulation results can be compared to the previous data. Also, there are possibilities of research collaboration with groups at UMass Medical School working on tuberculosis (TB). This collaboration would potentially allow for the GP-MSN-Rif complexes to be tested *in vitro* with TB infected macrophage cells and *in vivo* in a TB murine infection model.

Doxorubicin was chosen because it is a fluorescent cancer drug. Fluorescence is ideal for quantitative and qualitative microscopic analysis of glucan particles encapsulated formulations. Dox is also an ideal drug to study because of its anti-tumor activity. A long-term goal of the project is to demonstrate the delivery of glucan particle encapsulated Dox into macrophages and using the macrophages as Trojan horse carriers of the GP-MSN-Dox formulation into tumors following macrophage migration into tumors.

1.3.1.1 Rifampicin

Rif is a semi-synthetic antibiotic that belongs to the chemical group of rifamycins. Rif is the first antibiotic of the ansamycin family and is a first-line agent used in the treatment of tuberculosis (TB). The drug was isolated in 1959 by Sensi et al. from a strain of *Amycolatopsis mediterranei* and was introduced into therapy in 1962 (Sensi, Margalith, & Timbal, 1959). The antimicrobial activity of Rif is a direct result of its inhibition of bacterial RNA polymerase (RNAP). Rif binds to conserved amino acids in the active center of the enzyme and blocks transcription initiation. One limitation with the use of this drug is the resistance to Rif due to mutations of the amino acids that Rif binds to (Tupin, Gualtieri, Roquet-Baneres, Morichaud, Brodolin, & Leonetti, 2010).

In order to achieve enhanced uptake of Rif into target cells and to reduce the drug dosage, new targeted drug delivery methods have been studied, since the drug can be toxic in high concentrations. Nanoparticle and microparticle-based delivery vehicles have

been used for the delivery of Rif. These vehicles include liposomes, PLGA microparticles and nanoparticles, and dendrimers. In previous work, Rif was encapsulated in GPs to demonstrate targeted delivery to alveolar macrophages, the primary replication site of TB. In order to delay the release of the drugs from the microparticles, the pores of the GPs were sealed using an alginate or chitosan hydrogel. The hydrogel seal of the GPs was able to extend drug release for 24-72 hours. Also, it has been shown that the effect of GP targeted Rif delivery to macrophages enhances Rif antimicrobial effects. (Soto E. , Kim, Lee, Kornfield, & Ostroff, 2010). Limitations of these formulations were observed in this study due to low Rif loading and lack of control over timed release.

1.3.1.2 Doxorubicin

Doxorubicin (Dox), also commonly referred to as adriamycin or 14-hydroxydaunorubicin, is an anthracycline-type anti-tumor drug that acts against cancer cells. Clinical studies of Dox began in 1969 under the direction of Dr. Gianni Bonadonna of the Instituto Nazionale per lo Studio e la Cura dei Tumori in Milan, Italy (Bonadonna, Monfardini, De Lena, Fossati-Bellani, & Beretta, 1970). In the mid 1970s clinical trials began in the United States after the discovery of the drugs antitumor activity. Thus far, *Streptomyces peucetius* ATCC 27952 is the only known organism known to produce Dox. Doxorubicin is a popular cancer drug because it exerts antiproliferative activity on cancer cells via two different mechanisms. The two mechanisms are intercalation and enzyme inhibition which both result in DNA disruption and eventually cell death (Niraula, Kim, Sohng, & Kim).

Presently, Dox is an antibiotic widely used in cancer chemotherapy. However, there are a few limitations in the use of Dox as an antitumoral agent. The first limiting factor is the drugs chronic or acute cardiotoxicity. Cardio effects of Dox are expressed by changes in the electrocardiogram, which are generally reversible, but can cause a congestive heart failure resulting in death. The affinity of Dox towards negatively charged phospholipids could partially explain the cardiotoxic effect of the drug. Another limiting factor is the spontaneous or acquired resistance to the drug. The cause of this resistance is related to the modification of the cell membrane (Aubel-Sadron & Londos-Gagliardi, 1984).

2. Materials and Methods

Materials: All chemicals for the synthesis of MSN were purchased from Sigma Aldrich and Fischer Scientific and used as received. Glucan lipid particles (GLPs) and glucan particles (GPs) were prepared in the Ostroff laboratory using Baker's yeast (Fleishmans Baker's yeast, AB Mauri Food Inc., Chesterfield, MO, or from SAF-Mannan, Biospringer, Juno, WI). All materials for cell tissue culture experiments were purchased from Gibco Scientific or Fischer Scientific. The purity of rifampicin and doxorubicin drugs used for the evaluation of MSN samples was corroborated by measuring of the UV/Vis absorbance spectra of rifampicin (Appendix A) and the fluorescence excitation/emission spectra of doxorubicin (Appendix B).

Equipment: Spectrophotometric assays were measured with Safire Tecan 2 plate reader. Fluorescence microscopy images were obtained with a Zeiss Axiovert 200 microscope equipped with a Zeiss AxioCam HR CCD camera with 1300x1030 pixel resolution. GP/MSN samples were evaluated at a 100x magnification. Experiments with cells on 24-well plates were evaluated at a 20x magnification.

2.1 Synthesis of Mesoporous Silica Nanoparticles

Several classes of MSN were synthesized to have a collection of material with different functionalities. The different MSN compositions are listed in Table 1. All MSNs were made from commercially available materials with the exception of the fluorescent MSN, for which fluorescent-APTS (f-APTS) was synthesized.

Synthesis of Fluorescent-APTS (f-APTS):

Amino-propyltriethoxysilane (200 µL) was reacted with fluorescein isothiocyanate (FITC, 7.3 mg) in 1 mL of ethanol. The reaction mixture was stirred under nitrogen for two hours. The reaction mixture was stored at -80 °C until ready to use for MSN synthesis. f-APTS samples in ethanol were stored for no more than two weeks.

Mesoporous Silica Nanoparticles (MSNs):

A solution containing cetyl trimethylammonium bromide (CTAB, 3.5 g) in water (168 mL) and NaOH (2 M, 1.2 mL) was heated at 80°C and stirred vigorously until the solutes were dissolved. 24 mL of the CTAB solution was added to six different 50 mL centrifuge tubes. Each tube was placed in a hot water bath on a hot/stir plate and stirred vigorously. A solution containing the MSN reagents (tetraethylorthosilicate, TEOS or amino-propyltriethoxysilane APTS) was prepared as shown in Table 1. Once the solutions reached 80 °C the APTS/TEOS solutions were added and stirred at 80 °C for 15 minutes. 3-trihydroxysilylpropyl methylphosphonate (PO4) was added to and the solutions were left to incubate for 2 hours at 80 °C with stirring.

The solutions were cooled to room temperature and then centrifuged for 20 minutes. The particles were washed using 50 mL of methanol and centrifuged for an additional 15 minutes. The particles were left to dry overnight. The CTAB was extracted from the MSN by refluxing the particles (850 mg) in an acidic methanol mixture (90 mL of methanol and 5 mL of 12.1 M HCl) for 24 hours. The particles were then washed with 50 mL of methanol three additional times and left to dry overnight.

A negative TEOS control sample (MSN-7) was prepared by reacting TEOS (2.5 mL) in a solution containing only NaOH (no CTAB) at 80 ˚C for two hours with continuous stirring. The sample was then cooled to room temperature and placed in the negative 80 ˚C freezer before being lyophilized. The product was washed three times with 50 mL of water and three times with 50 mL of methanol. The final product was left to dry overnight at room temperature.

2.2 Synthesis of Cationic Glucan Particles

Three 15 mL tubes were prepared with 15 mg of GPs. The particles were resuspended in 10 mL of deionized water. The samples were centrifuged and the water was discarded. 600 µL of a 1 mg/mL solution of potassium periodate and 2.4 mL of water was added to the samples and the mixture was left stirring in a dark room at room temperature over night. The solutions were centrifuged and the supernatant was discarded. Each sample was then washed three times with water. Each sample was resuspended in a specific amount of polymer and water, as indicated in Table 2. The mixtures were stirred at room temperature for 24 hours. Sodium borohydride (0.45 g) was then added to each mixture and the mixtures continued to be stirred at room temperature for another 24 hours. Sodium borohydride (0.45 g) was added again to each mixture and the samples continued stirring at room temperature for additional 24 hours. The mixtures were centrifuged and the supernatant was discarded. The samples were washed three times with water and 2.5 mL of tris buffer was added. The mixtures were stirred for 30 minutes and then washed three more times with water. The samples were resuspended in

70% ethanol and incubated at -20 ˚C for at least three hours. Finally, the particles were aseptically washed three times with 0.9% saline and resuspended in 0.9% saline. The particles were then counted with a hematocytometer, and the solution was adjusted to a concentration of 1 x10^8 particles/mL.

2.3 Loading of GP and GLP with preformed f-MSN

Four samples were prepared using 1 mg/mL of f-MSNs in PBS (samples MSN-4 and MSN-5, Table 1. A 100 µg/mL dilution of each MSN sample in PBS was prepared. 5 µL of MSN samples was added to magnetic GPs and GLPs. Each sample was mixed with a blunt heat-sealed pipet tip, centrifuged, and incubated at room temperature for one hour. After the incubation period, the samples were placed in the -80 ˚C freezer for approximately five minutes and then lyophilized. Each sample was water pushed by adding 5 µL of water, mixing with a blunt pipet tip, centrifuging, incubating for one hour at room temperature, and lyophilizing. The samples were resuspended in 1 mL of 0.9% saline and the GPs were magnetically purified from the unbound MSN.

The second sample was resuspended in 1 mL of phosphate buffer (no salt), with a pH of 6.5. Zymolyase (50 mg) was dissolved in 0.5 mL of the phosphate buffer and the solution was added to the GLP sample. The sample was incubated at 45 ˚C for 1 hour. After the incubation period the sample was centrifuged at 10000 rpm for 15 minutes. The supernatant was discarded and the sample was washed two times with 1 mL of water. The product was lyophilized and evaluated by IR, DLS/Z-potential, and Dox binding.

2.4 GLP *in situ* synthesis of MSN

MSN synthesis inside glucan lipid particles (GLPs) was attempted using fluorescently labeled APTS to monitor the formation of MSN inside GLPs by microscopy. Optimal loading conditions (solvent, MSN reagent concentrations) were determined using f-APTS before attempting GLP *in situ* synthesis of MSN with non-fluorescent orthosilicates.

2.4.1 MSN Synthesis with F-APTS

Loading of MSN starting materials (TEOS, f-APTS) was evaluated using organic solvents that efficiently penetrate the pores of GPs and GLPs. Miscible solvent mixtures were prepared as shown in Table 3

GP or GLP blanks (10 mg) were mixed with 50 μL of liquid from each of the solutions shown in Table 3. The samples were mixed using a blunt pipet tip, sonicated, and incubated at room temperature for 1 hour. The samples were then centrifuged, the supernatant was discarded, and the samples were lyophilized for four hours. A CTAB and NaOH solution was prepared using 0.5 g of CTAB, 2.5 mL of water, and 70 μL of 5 M NaOH and heated to 80 ˚C. CTAB/NaOH solution (50 μL) was added to each sample and mixed immediately with a blunt pipet tip. The samples were incubated at 80 ˚C for two hours with periodic mixing. After the incubation period, each sample was resuspended in 1 mL of ethanol until the supernatant was clear. The samples were then lyophilized. Particles were evaluated by fluorescence microscopy for evidence of f-APTS trapping inside GPs or GLPs.

2.4.2 *In situ* MSN Synthesis With Optimal Loading Conditions

FITC (3.6 mg) was dissolved in 0.5 mL of ethanol. 60 μL was added and the reaction was stirred for two hours in the dark. The TG loading solution was prepared. The solution contained 900 μL of TEOS, 100 μL of FITC-ATPS, and 90 μL of geraniol. Two 1 mL centrifuge tubes were prepared with 100 mg of the GLP sample. 500 μL of the TDG solution was added to each tube. The solutions were mixed using a blunt pipet tip and cup sonicated. The samples were incubated at room temperature for 1 hour. The samples were then centrifuged for 2 minutes at 3000 rpm and the supernatant was discarded. The samples were lyophilized for 4 hours. A CTAB and NaOH solution was made containing 0.5 g of CTAB, 2.5 mL of water, and 70 μL of 5 M NaOH and was heated to 80 ˚C. 500 μL of the CTAB/NaOH solution was added to each tube and immediately missed with the blunt pipet tip. The samples were incubated for two hours with periodic mixing. After the incubation period, 1 mL of ethanol was added to each sample, the samples were then cup sonicated, centrifuged and the supernatant was discarded. Each sample was then resuspended in 1 mL of ethanol and centrifuged until the supernatant was completely clear. Finally, the samples were lyophilized.

The first sample was evaluated for particle hydration in water and the fluorescent sample was evaluated at 100x. The particles were sterilized in 1 mL of 70% ethanol and the sample was aseptically washed. The particles were counted and 1×10^8 part/mL dilutions were prepared.

2.4.3 *In situ* synthesis of non-fluorescent MSN in GLPs

Loading solutions of TEOS, APTS, ethanol and geraniol were prepared in the concentrations shown in Table 4.

GLP samples were prepared at the 50 mg scale. 250 µL of the indicated loading solution was added to each tube. The samples were mixed using a blunt pipet tip and sonicated. The samples were then incubated at room temperature for 1 hour. The samples were then centrifuged, the supernatant was removed, and they were lyophilized for 4 hours. A CTAB/NaOH solution was prepared using 0.5 g of CTAB, 2.5 mL of water, and 70 µL of 5 M NaOH and was heated to 80 ˚C. 500 µL of the CTAB/NaOH solution was added to each sample and immediately mixed with a blunt pipet tip. The samples were incubated for 2 hours at 80 ˚C with periodic mixing. After the incubation period 1 mL of ethanol was added to each sample and sonicated. The samples were centrifuged; the supernatant was discarded and once again the sample was resuspended in 1 mL of ethanol. After removing the supernatant, the samples were resuspended in a 1 mL mixture of 900 µL of MeOH, 50 µL of water and 50 µL of HCl. The CTAB was extracted from each sample by refluxing the sample overnight. Once the CTAB was removed, the samples were washed three times with methanol and the pellet was left at room temperature to dry.

2.5 Binding of MSN To Surface Derivatized GPs

MSN suspensions and GP particle suspensions were mixed in Eppendorf tubes. In a typical experiment, samples containing $1\text{x}10^6$ particles of either a cationic GP surface

(i.e. 25 kDa PEI-GP) and a negative control (neutral GP) were evaluated with different MSNs. The MSN concentration was varied from 0 to 0.2 mg/mL. 0.9% saline was added to bring the total volume of all samples to 100 uL. All samples were incubated in the dark, at room temperature for at least two hours with constant stirring. Unbound MSN and glucan particle bound MSN fractions were purified by two methods: (1) standard centrifugation and (2) pelleting through a 20% sucrose cushion. In the first method, samples were centrifuged for 5 minutes at 10000 rpm. The supernatant was transferred to a 96-well plate and the pellet was washed with 100 μL of 0.9% saline. The samples were once again centrifuged and the supernatant was transferred to the 96-well plate. The samples were then resuspended in 0.9% saline and the pellet was transferred to the plate. In the sucrose cushion method, the samples were carefully layered over a 100 μL 20% sucrose in 0.9% saline to create a two phase system with the sucrose cushion solution underneath the original solution containing the GPs and MSN samples. Each sample was centrifuged for 10 minutes at 3000 rpm and the supernatant was transferred to the 96-well plate. The samples were then resuspended in 200 μL of 0.9% saline and centrifuged for 5 minutes at 10000 prm. The supernatant was transferred to the plate and the samples were resuspended in 200 μL of 0.9% saline. The pellet was then transferred to the 96-well plate. The FITC fluorescence was measured and the percent of sample bound to the GP pellet was evaluated. The samples with higher binding capacity and the controls were also evaluated under the microscope at 100x.

2.6 Mesoporous Silica Bound Drugs

2.6.1 Drug Binding to pre-formed MSN

All MSN samples listed in Table 1 were evaluated for binding of payload drugs. MSN suspensions (4 mg) and payload molecules (0-1 mg) were incubated in 1 mL of DMSO or water overnight at room temperature. The samples were then centrifuged and the supernatant was transferred to an Eppendorf tubes. The solvent/MSN pellets were lyophilized before being resuspended in 250 µL of water. The samples were then centrifuged and the supernatant was collected in order to measure the released drug. The pellets were washed two more times with water and then resuspended in 1 mL of methanol. The samples were left to incubate overnight as room temperature. The samples were centrifuged and the supernatant was collected in order to measure the amount of released drug.

Additionally, the MSN loading was evaluated using hydrodynamic volume Loading. In this method, MSN suspensions (100 µL, 20 mg/mL) were transferred in Eppendorf tubes. The samples were centrifuged and the excess solvent was removed before being lyophilized. Rif and Dox solutions were added to each sample and the exact volume required to swell the MSN pellet was recorded. The samples were incubated overnight at room temperature and then lyophilized. Each sample was washed with 1 mL of water until the supernatant became clear. The supernatants were collected in order to measure the unbound Dox or Rif. The samples were then resuspended in 1 mL of methanol and incubated overnight at room temperature. The samples were then

centrifuged and the methanol supernatant was collected in order to measure the bound Dox or Rif.

2.6.2 Drug Binding to GLP-MSN

Water-soluble drugs were evaluated for uptake in water and in a water/DMSO 50:50 mixture. Water insoluble drugs were evaluated for particle uptake in DMSO and in a water/DMSO 50:50 mixture. GLP-MSN samples ($1x10^6$ particles) or negative GLP control, drug solution, and solvent were mixed in order to obtain a final volume of 100 µL. All samples were incubated at room temperature for at least an hour. After the incubation period the samples were centrifuged for 3 minutes at 10000 rpm and 90 µL of the supernatant was transferred to a 96-well plate in order to measure the unbound payload. The samples were washed in the original solvent mixture used to dissolve the payload drug. Each sample was vortexed and centrifuged at 10000 rpm for 3 minutes. The supernatant was transferred to a 96-well plate and another 90 µL of the solvent was added to each sample. The samples were vortexed, cup sonicated, and 100 µL were transferred to the 96-well plate. The fluorescence and UV/Vis or absorbance of each sample was measured. The pellets were then transferred back into the Eppendorf tubes and centrifuged. The solvent was removed and the samples were resuspended in in 100 µL of 0.9% saline. The samples were then evaluated with a fluorescent microscope for evidence of drug binding inside GLPs.

2.7 Drug Release Assays from MSN

Indicated amounts of Dox-MSN samples were suspended in solutions of PBS, Acetate Buffer, 10% FBS in PBS, 10% FBS in acetate buffer, and Ethanol. Five samples were created in each solution. Each sample was left to incubate in the dark for a set period of time: 1 hour, 3 hours, 24 hours, 48 hours, or 72 hours. At the end of the incubation each sample was centrifuged at 10000 rpm, the supernatant was removed to a 96 well plate. The Dox fluorescence was then measured using the parameters of wavelength: 470 nm and emissions: 550 nm.

2.8 Analytical methods for characterization of MSN and GPs

2.8.1 Fourier-transform Infrared (FT-IR) spectroscopy

IR spectra were obtained with a Nexus FT-IR spectrometer using the attenuated total reflectance (ATR) technique. For each sample 16-128 scans were collected with a 4 cm^{-1} resolution. The scan range was from 4000 to 500 cm^{-1}.

2.8.2 Dynamic Light Scattering (DLS) and Zeta Potential Measurements.

Size and zeta potential of MSN samples, and zeta potential of MSN-GP samples were determined with a Malvern Zetasizer Nano-ZS (Malvern Instruments, Worcestershire, UK). Solvents and buffers were filtered through a 0.22 μm filter before sample preparation. A suspension of particles (1 mg/mL for MSN samples, $2x10^{6}$ particles/mL for GP samples) was diluted in 1 mL of 20 mM Hepes buffer, vortexed and transferred to a 1 mL clear zeta potential cuvette (DTS1061, Malvern). Zeta potential was

collected at 25 °C from -150 to +150 mV. The results are the average of 30 measurements collected and analyzed with the Dispersion Technology software 4.20 (Malvern) producing diagrams of zeta potential distribution versus total counts. DLS measurements were obtained from samples in the same zeta potential cells at 25 °C. The average of 20 measurements was collected in the size range from 1 nm to 10000 nm. The data was analyzed with the Dispersion Technology software producing histograms for the particle size versus % intensity.

2.8.3 Flow Cytometry FACS

Flow Cytometry (FACS) measurements were obtained with a Becton Dickinson FACS Calibur instrument (BD, Franklin Lakes, NJ). Samples were prepared for FACS analysis by binding of 10 uL of 0.5 mg/mL Dox-MSN to 2×10^6 particles. The samples were washed from unbound Dox-MSN and resuspended at 2×10^6 GP/mL in PBS. Unmodified GPs were used as negative controls and fluorescein labeled GPs as the positive control. The particles were analyzed with an FL2 laser at 550 nm by collecting an average of 15000 measurements. Gating and analysis was performed using FlowJo 6.4.2 software.

2.10 Dox-MSN/GP cell delivery

Saline, GP particle suspensions, and Dox-MSN suspensions were combined in indicated concentrations. GPs were used at 10 particles per cell, while Dox-MSN was used from 5×10^{-5} to 5 mg/mL concentrations. The Dox/GP ratio used was 5×10^{-7} mg to 0.05 mg Dox per 1×10^6 GPs. Different concentrations and samples of both MSN and GP

particles were used. 100 μL of solution was created for each cell plate. The mixture was then incubated at room temperature for one hour. The samples were then washed two times with 0.9% Saline. DMEM was added to each tube and the mixture was slowly mixed with a pipette. The samples were then added to the indicated cells. To test for Dox-MSN uptake the plates were incubated for 3 hours at 37 ˚C. The cells were then fixed with 1% formalin in order to observe GP mediated uptake of Dox-MSN. To test for cell growth and cell viability the samples were incubated for 3 hours, 24 hours, 48 hours, or 72 hours. The optimal effect was observed at 48 hours so additional experiments were processed at 48 hours to collect the cells and to count them.

Cell culture experiments were repeated for cell lines B6 (a macrophage cell line with glucan receptors), 3T3-D1 (3T3 cell line modified to express glucan receptors), and 3T3 (cells with no glucan receptor). For evaluation of growth arrest the cells were processed after a 48 hour incubation at 37 °C. First, the medium was removed and the cells were washed with sterile PBS once. Then 250 μL of sterile PBS and 25 μL of 1% trypsin-EDTA were added to each well to remove the cells from the well. The cell suspension was transferred to Eppendorf tubes and centrifuged at 1000 rpm for 10 minutes. The PBS was carefully removed and the cells were resuspended in 100 μL of 2% trypan blue in PBS. The cells were counted with a hematocytomer and the percentage of cell growth was normalized relative to the count of cells in a well incubated with only DMEM and 0.9% saline.

2.9   Biological assays for evaluation of drug-MSN/GP

2.9.1 Minimum inhibitory concentration (MIC) assays

100 μL of 2x Lysogeny broth (LB) was added to row A of a 96 well plate containing *E. coli* while 100 μL of 1x LB was added to all other wells. 100 μL of a sample was then added to the wells in row A. A serial dilution was then created with a multi-channel pipette by transfer 100 μL of solution from row A to row B and so forth. 100 μL is removed from row H and discarded. A solution of 1:100 *E. coli* in 1x LB is then added to each well starting with row H. Optical Density was then recorded at 650 nm using a microplate reader. The plate was then incubated overnight at 37 ˚C. Optical Density was again recorded at 650 nm using a microplate reader. 40 μL of 0.05% resazurin (7-hydroxy-3H-phenoxazin-3-one 10-oxide) was then added to each well. The sample was incubated at 37 ˚C until the control well showed a change in color from blue to pink; at this point a picture was taken.

3. Results and Discussion

Methods to prepare glucan particles (GPs) containing mesoporous silica nanoparticles (MSNs) for small drug molecule targeted delivery to macrophages were completed. It was the goal of this project to synthesize GPs containing MSNs to create a delivery agent that benefits from the macrophage targeting capabilities of glucan particles and small drug molecule binding capacity of MSNs. The project began with the synthesis of seven different MSN samples. MSNs were then combined with GPs in three different

synthetic methods; (1) encapsulation of MSN inside of the GPs, (2) *in situ* synthesis of MSN within the GPs, and (3) binding of the MSNs to the exterior of the GPs. The drugs doxorubicin (Dox) and rifampicin (Rif) were bound to the GP-MSNs and the complexes were evaluated for its antimicrobial activity (Rif samples) or effect on drug delivery and growth arrest of 3T3-D1 and 3T3 cells.

3.1 Synthesis and characterization of MSNs

MSNs are used in the delivery of drugs and controlled release. By developing MSN samples with different attached charged groups, it is possible to compare the delivery and release of varying MSNs with the drugs doxorubicin and rifampicin. In the infancy of this project, seven different samples of MSN were developed as indicated in Table 1. The MSN-1 sample was built as the TEOS standard while the other MSN samples contain either phosphate or amine or both groups to have a surface charge inside of the pores that will enhance binding of drugs by electrostatic interaction. The MSN samples were characterized by Fourier Transform Infrared Spectroscopy (FT-IR), zeta potential, and dynamic light scattering measurements. The samples labeled with f-APTS were also evaluated by fluorescence microscopy.

Formation of the CTAB micelle is critical to MSN synthesis as the micelle acts as a template to produce a highly porous material. In the absence of this template the orthosilicate compounds decompose in water to form silicon dioxide (sand). A control sample (MSN-7) was prepared from TEOS reaction in water in the absence of CTAB. Comparison of MSN-7 and MSN-1 (sample density, aggregation, IR and drug adsorption) confirmed the successful formation of a porous material for MSN-1.

FT-IR of MSN before and after CTAB extraction was collected to evaluate complete removal of CTAB from the MSN/CTAB mixture. During the synthesis of MSN, CTAB was extracted from the samples creating completely porous nanoparticles. Figure 10 shows the IR spectra of MSN-1 before and after the CTAB extraction. The spectrum of the MSN-1 sample with CTAB displays a hydroxyl group at 3373 cm^{-1}, this hydroxyl group belongs to the CTAB. The spectrum of the MSN-1 sample without CTAB shows no peak within that range proving the successful extraction of CTAB from the sample.

The IR spectrum of MSNs show absorption bands in the range of 3750-3000 cm^{-1} due to the silanol groups. Surface functionalization of MSNs by the co-condensation method provides with additional vibrational bands. For examples, surface functionalization of the outer hydroxyl groups with APTS to form Si-O-Si bonds leads to a decrease in the silanol absorption band at 3750-3000 cm^{-1}. The most significant band of the TEOS/APTS and TEOS/APTS/PO4 samples correspond to the CH_2 asymmetric bending at 2933 and 2871 cm^{-1} and the NH_2 stretching mode at 3375 cm^{-1} ((Zhang, Zhi, Jiang, Zhang, Wang, & Wang, 2010). These bands are exhibited in the IR spectrums shown in Figure 11.

The low intensity of most of the IR peaks did not allow for the complete characterization of the MSN samples. Clear evidence of successful synthesis was provided by measuring the zeta potential of each MSN sample.

Zeta potential is a technique that measures the outer boundary layer of ions formed between the solvent and a particle. This outer layer is affected by the net charge distribution of ions in the particle. The zeta potential results shown in Table 5 show clear evidence of the surface functionalization of MSN nanoparticles. MSN-1 prepared with TEOS has an almost neutral zeta potential. Samples containing amine groups (MSN-3, MSN-4) show a significant shift to a positive zeta potential (cationic MSN), while samples with phosphate (MSN-2) show a significant shift to a negative zeta potential (anionic MSN). The MSN-5 and MSN-6 samples containing both phosphate and amine groups show that the MSN nanoparticles are anionic, which is expected as the phosphate compound (PO4) was selected to have a longer alkyl chain spacer than the amine compound (APTS). This was done following previous work (Meng, et al., 2010) showing that the PO4 compound stabilizes the MSN by preventing particle aggregation due to amine hydrogen bonding between MSN nanoparticles in samples like MSN-3.

Based on Table 5, the particle with the greatest binding capacity is the MSN bound with TEOS/APTS/PO4 because the zeta potential value exceeds -30 mV. Zeta potential has the limitation of effect of particle aggregation. Nanoparticles that tend to aggregate and settle will lead to a shift of zeta potential to a neutral value even if the sample has a high density of charged (either anionic or cationic) surface groups.

Dynamic light scattering (DLS) measurements of the MSN samples collect information of particle size and particle size distribution. Table 5 shows both the average particle size and polydispersity index (PDI). PDI determines how homogenous or heterogeneous the sample is. The PDI is determined on a scale from 0 to 1, 0 being

completely homogenous and 1 being completely heterogeneous. All samples shown here have a high PDI, this implies a high level of heterogeneity. The amine particle size shown in Figure 13 represents the most common particle size value. However, the nanoparticles assume a broad range of sizes. Microscopic evaluation of fluorescent MSN (Figure 14) confirmed the heterogeneity of particle size of all samples.

3.2 GP and GLP loading of pre-formed MSNs

The first approach to incorporate pre-formed mesoporous silica nanoparticles inside of the glucan particles was to load the MSN samples directly into the GPs. The loading of nanoparticles into glucan particles had been completed previous to this project allowing for a comparative reference. Nanoparticles of less than 40 nm in diameter (i.e. magnetic iron oxide NPs of 10 nm in diameter, quantum dots, polystyrene nanoparticles) have been successfully loading inside the hollow cavity of GPs and trapped either by aggregation of nanoparticles or trapping of derivatized nanoparticles by crosslinking with a polymer by electrostatic interaction (Soto & Ostroff, Encapsulation of Nanoparticles Inside Yeast Cell Wall Particles for Receptor-targeted Drug Delivery, 2010). However, experiments failed when attempting to reiterate the previous YCWP delivery system with GP loading of pre-formed MSNs. Two major issues contributing to the failure of loading pre-formed MSN into GPs was MSN particle size and heterogeneity. The significantly larger MSN nanoparticle size of 50-100 nm resulted in a small amount of MSNs being trapped inside of the GPs. In order to visualize the results, we used MSN/fAPTS but microscopy images showed approximately 1 in 100 particles loading into the GPs. In conclusion, the MSN samples did not have enough material of the required size to get

inside of the GPs so further loading strategies were undertaken in order to synthesize a successful drug delivery system. Next, we loaded starting materials for MSN and carried out the synthesis of MSN inside of the GPs.

3.3 GLP *in situ* synthesis of MSNs

The MSN was synthesized inside of the GLP. By adding TEOS/APTS with geraniol/ethanol to the GLP the TEOS/APTS got trapped inside of the GLP. Geraniol/ethanol mixture was used as solvent as the silicate compounds react with water, the common solvent for GP payload loading. The resulting product of water and TEOS would generate sand (as proved with MSN-7 control sample). Once the TEOS/APTS is inside of the GLP, MSN was synthesized by adding CTAB aqueous solution to the GLP and incubating at 80°C. GLP *in situ* synthesis of MSNs is a preferable drug delivery agent because the MSN is protected by the glucan particle.

In the first generation of GLP-MSN samples, fluorescent APTS (fAPTS) was used to monitor the formation of MSN inside the hollow cavity of the GLPs. The microscopic images shown in Figure 15 shows that the MSN was successfully synthesized inside of GLPs. The figure is set up with the bright field image on the far left, the middle image is of the fluorescence, and the third image is an overlay of the two images. This picture shows the GLPs in the bright field image and the MSN in the fluorescent image, by overlaying the two pictures in the third image it is possible to see that the MSNs are within the GLPs. This process qualitatively proves that MSN can be made with in the GLPs.

Following optimization of MSN *in situ* synthesis with f-APTS, we focused our efforts on synthesizing GLP-TEOS/APTS/PO4 as this sample is expected to have better binding capacity for Dox than other GLP-MSN samples. However, the drug binding capacity bound inside of GLP-MSNs is not significantly higher than the GLP-TEOS or the empty GLPs, which was used as the negative control. These results indicate that most of the Dox samples bound to the glucan particle's lipid layer rather than the MSN.

The solvent used in loading drugs into the GLP-MSNs plays a significant role in the amount of drug bound to the GLP-MSNs. In order to load GP-MSNs with drug the particles must swell. Although water is an excellent solvent in swelling GPs it does not have an effect on MSNs. MSNs tend to aggregate in the presence of water and pore permeation and encapsulation of the drug is therefore reduced. On the other hand, DMSO easily swells the MSNs but if the concentration of DMSO exceeds seventy percent it will degrade the GLPs. In an attempt to successfully load drug into the GP-MSNs, DMSO with a concentration of fifty percent was used as a loading solvent. The results, as shown in figure 16, display a significantly larger amount of drug bound to different GLP-MSN samples loaded in 50% DMSO in comparison to water.

Figure 17 shows the maximum binding capacities at different concentrations of Dox. Overall the highest binding was seen in the control sample, containing no MSN. This was believed to have occurred because the lipid layer is still intact with the control GLPs, while the lipid layer in the process samples was probably no longer intact. Since it was difficult to preserve that layer and achieve high binding with the GLP-MSN

complexes it was determined that it would be more efficient to attach the MSN particles to the outside of the GPs rather than the inside.

Once we demonstrated that building the MSN inside of the GLP was going to have a limitation regarding drug binding we followed up with a strategy with which we attached MSN containing the drug to the outer surface of the GP.

3.4 Evaluation of MSN binding to the outer surface of GPs

Specific MSNs were developed for controlled release and drug delivery systems. Surface functionalized MSNs display well-defined surface properties for site-specific delivery and hosting molecules with various size, shapes, and functionalities. In the case of this project, MSNs were used in the drug delivery of doxorubicin (Dox) and rifampicin (Rif). By covalently binding to the drugs, MSNs are capable of delivering both drugs to cells containing glucan receptors.

Pre-formed MSN nanoparticles were first loaded with the payload drug, evaluated for binding capacity and release under different pH conditions, and finally a biological assay was carried out for the free drug-MSN sample or bound to the surface of glucan particles.

3.4.1 Rif-MSN

Two different MSN samples, MSN-1 and MSN-6, were used to look at the titration of Rif and observe how much Rif bound to the MSN. The results, displayed in

figure 18, show that the cationic MSN had a higher binding capacity. The experiment was then repeated at 50% loading using MSN-1, MSN-2, MSN-3, and MSN-6. The results can be seen in Figure 19. In an attempt to bind as much Rif to MSN as possible, we prepared the samples with a high concentration of Rif since a saturation point was not reached in the titration experiment shown in Figure 18. After the evaluation of Rif binding and release from MSN, the samples were tested for their effect on inhibiting the growth of *E. coli*.

The Minimum Inhibitory Concentration (MIC) is the lowest concentration of an antimicrobial that it takes to kill a microorganism. In the case of this project, the MIC is determined to be the lowest concentration of Rif-MSN that is needed to kill more than 90% of the *E. coli*. Referring to Table 6, Rif-MSN 1 had no effect on the *E. coli*. The reason why the *E. coli* remained unharmed is because MSN-TEOS has high aggregation in water making it nearly impossible to resuspend. The most successful Rif-MSN was sample 4 because the MSN-TEOS/APTS/TEOS has a MIC at 3.125 mg/mL. The MSN-5 (no Rif) was used as MSN control, which is predicted to not have an effect on the *E. coli* because it is not a toxic material. Looking at Table 6, there is a false positive result showing that the MSN control is killing the *E. coli*. It is possible to receive false positives because MIC assay calculations are based from light absorption readings. However, absorption is sensitive to the presence of particles; a high concentration of particles cause light scattering so the sample absorbance or optical density is not the only measurement.

In reaction to the false positive results, a secondary assay was compared to the absorption measurements in order to determine which Rif-MSN samples are actually

killing *E. coli*. Resazurin (7-hydroxy-3H-phenoxazin-3-one 10-oxide) is an oxidation-reduction indicator used in cell viability assays for bacteria and mammalian cells. By adding resazurin, one can observe the dramatic change in color between the dead and alive *E. coli*. As observed in Figure 20, the TEOS control shows no evidence of dead *E. coli* proving that the absorption of the MSN-TEOS control is a false positive. However, all other results hold true to the absorption results (Carter, Gaspar, & Leise, 1955).

Rif-MSN samples were not evaluated for binding to the GP surface and GP mediated delivery of Rif-MSN into cells expressing glucan receptors. The reason why these experiments were not pursued is because the original concentration of nanoparticles was 50 mg/mL, which is significantly large. The lowest possible concentration of Rif-MSN that will have an effect on killing the *E. coli* is 3 mg/mL, which is still a very large concentration of nanoparticles. This concentration is not ideal when using GP because only a very small percentage of the Rif-MSN will bind to the GP and will have little to no affect at all on the *E. coli*. With such little drug concentration the GP will deliver the Rif-MSN into the cells but it will take a long time to see any inhibition in *E. coli* growth.

3.4.2 Dox-MSN

The binding capacity of Dox to MSN plays an extremely important role in the inhibition of cell growth in a specific amount of time. A higher percentage of Dox bound to MSN is a result of binding to an anionic MSNs. Experimentally; two MSNs were created and compared. The first MSN was attached to a TEOS group, resulting in a neutral charge. The second MSN was attached to a TEOS/APTS/PO4 group, which has

the negative phosphate groups more accessible for binding. By adding a charge to the MSN, a significantly greater percentage of Dox bound to the MSN. These results prove that a negatively charged group attached to MSN increases the amount of drug being carried.

As shown in Figure 21, the amount of Dox that bound to MSN-TEOS/APTS/PO4 was approximately 6 fold higher than the amount of Dox bound to MSN-TEOS. Dox holds a positive charge that is highly attracted to negatively charged particles. A negatively charged phosphate group was added to the MSN-TEOS/APTS in order to the give the MSN an overall negative charge.

The kinetics of Dox release from Dox-MSN samples was evaluated at different pH conditions. It is expected the samples to be stable in PBS (pH 7) and to show an increase in Dox release rate with low pH. This ideal release behavior would facilitate drug endosomal release upon uptake of the Dox-MSN-GP conjugates by cells. As seen in Figure 23, the samples show a slightly faster release at pH 5 or pH 2 relative to pH 7. However the amount of Dox release over 60 hours is only 10% of the original input. Samples were evaluated over longer periods of time (up to 7 days) without a significant increase in Dox release. This is likely the result of the MSN pores not allowing for efficient drug diffusion of the drug out of the pores when placing the MSN sample in aqueous solutions. Similar effect as the one shown in Figure 23 was observed for samples incubated at the same pH values with 10% fetal bovine serum (FBS).

Following optimization of Dox binding to MSN and evaluation of Dox release, the Dox-MSN samples prepared with MSN-6 were evaluated for binding to GPs and targeted cell delivery.

Dox-MSN samples were bound to two different GPs (neutral GPs and 25 k PEI-GP) and the binding was evaluated by FACS, zeta potential, and fluorescent microscopy.

Measurements of the zeta potential provided clear evidence that the Dox bound inside of the MSN. MSN samples were loaded with Dox in DMSO and then washed with water to remove Dox bound on the surface. This can be concluded because the zeta potential curve of MSN only had a very slight shift to the left when bound with Dox as shown in Figure 24. If the Dox had indeed bound to the outside of the particle than there would have been a very significant shift in the zeta potential curve.

The Dox-MSN samples were then bound to glucan particles. Figure 25 shows that 25 kPEI-GPs have a positive zeta potential. When Dox-MSN is bound with the 25k PEI-GP the zeta potential shifts to the left. Based on this observation, one can conclude that the Dox-MSN is bound to the surface of the GPs. The presence of only one peak for the DoxMSN-25kPEI-GP sample and microscopic evaluation confirm the preparation of samples that are free of unbound Dox-MSN.

Figure 25 also shows the zeta potential of GPs and GP conjugated with Dox-MSN. GPs have a neutral zeta potential. The magnitude of the shift for the Dox-MSN/GP sample is less than 10 mV relative to the zeta potential of GP. In comparison the shift for

the Dox-MSN/25kPEI-GP is almost 50 mV from the original zeta potential of 25kPEI-GP. This confirms that the Dox-MSN is effectively bound to the 25k PEI-GP, but not to the neutral GP. In theory, there should not be a shift in the zeta potential values when attempting to bind Dox-MSN with a neutral GP. The reason why the peak shifts slightly to the left is because of unavoidable experimental error. In order to wash the non-bound nanoparticles from a mixture of glucan particles and nanoparticles the mixture is centrifuged and the nanoparticles should remain in suspension. However, GPs act as a barrier to the nanoparticles as they attempt to resuspend in solution because the size of GPS are significantly larger than MSNs. The nanoparticles remained trapped under the GPs so the GP pellet can never be washed purely. Over time, as the GPs hold the MSNs down, the particles will eventually bind.

In addition to the zeta potential measurements, FACS analysis and fluorescent microscopy confirm more selective binding of Dox-MSN-6 to 25k PEI-GPs over the GP control.

As seen in Figure 26, the plot of Dox-MSN and 25 kPEI-GP shows one distinct peak. This peak represents a homogeneous sample and shows that all of the GPs are fluorescent. In order for the GPs to be fluorescent there must be at least one Dox-MSN attached to it.

Figure 26 also displays a plot of Dox-MSN and GP, which consists of a few different peaks. These peaks represent a heterogeneous sample and can be a result of experimental error or Dox-MSN binding to the residual chitosan in glucan particles.

When the mixture of GP and Dox-MSN is washed ideally the nanoparticles are suppose to suspend in the liquid leaving a pellet of GPs. However, the size of the GPs trap the nanoparticles causing the remaining pellet to be slightly impure. Another explanation for the multiple peaks could be the positively charged chitosan groups in glucan particles. GPs consist of 1% cationic chitosan groups that are attracted to the negative charge in Dox-MSN.

The binding of Dox-MSN to GPs was also confirmed by fluorescence microscopy (Figure 27). Imaging the samples for Dox fluorescence at the same image acquisition gain it clearly shows a brighter sample for the Dox-MSN bound to 25k PEI-GP compared to the neutral GP. In the case of neutral GPs the fluorescent Dox-MSN bound to the particles is minimal and can only be seen with high exposure times (10-15 sec) or the Dox-MSN is present in the particles as large aggregates not associated with glucan particles.

Following the characterization of the Dox-MSN-GP samples we tested the samples for efficiency to deliver Dox into NIH-3T3-D1 cells. This cell line has been genetically modified to express glucan receptors and efficiently phagocytose GPs.

In Figure 28 the GP mediated delivery of Dox is observed in 3T3-D1 cells after three hours of incubation. However, those same results are not shown with the Dox-MSN sample. The reason why these results differ are because the GPs are mediating delivery but at three hours there is not enough time for the nanoparticles (free Dox-MSN) to be internalized by cells through different particle uptake mechanisms. However, at 24 hours

there is much less difference in the fluorescence between samples delivered with and without GPs as there has been enough time to for endocytosis of free MSN.

Once shown that the Dox can be delivered into the cells using the MSN-GP we evaluated the effect of the these Dox samples on cell viability. At high Dox-MSN concentration it was possible to show complete inhibition of 3T3-D1 cell growth. However, at this concentration Dox-MSN delivery was not mediated by glucan particles. A Dox-MSN titration allowed to identify optimal conditions showing GP mediated delivery of Dox-MSN into cells. The experiments were done following two procedures. In the first method, the Dox-MSN/GP samples were added to cells and incubated for 3 hours. After this 3 hour incubation the DMEM medium was removed from the cells and fresh DMEM added. The DMEM collected after 3-hour incubation ("supernatant") was transferred to another well and the cells incubated for additional 48 hours. This strategy allowed for evaluation of the effect of sample internalized by cells after 3 hours (minimum time required for efficient GP uptake by 3T3-D1 cells) and also evaluation of effect of Dox-MSN or Dox-MSN/GP sample remaining in the medium after the 3 hour incubation. In the second method the medium was not changed until 24 hour incubation allowing for uptake of GPs, but also likely for uptake of free Dox-MSN or free Dox by other uptake mechanisms.

The results shown in Figure 29 ("supernatant") and Figure 30 (3 hour incubation) show the effect of glucan particle mediated delivery to cells at low Dox-MSN concentration. At this low concentration ($5e^{-5}$ mg of Dox-MSN per $1x10e^{6}$ GPs) it was not possible to effectively kill the cells, but a significant (50%) effect on growth arrest

was measured for Dox-MSN delivered via 25k PEI-GP samples compared to GP or free MSN. The Dox-MSN delivered by 25 k PEI-GP shows a clear effect after 3 hour incubation and there is not enough free Dox or free Dox-MSN remaining in the supernatant to show growth arrest.

There is no difference in cell growth with the supernatant because there was 100% cell growth at a low concentration of Dox-MSN.

When the media (DMEM) was changed at 3 hours you can observe a significant difference in cell growth for 25k PEI-GP. This information demonstrates that 25 kPEI-GP is binding with Dox-MSN at concentration 0.0005 mg/mL.

Samples incubated for 24 hours (Figure 31) did not show a clear effect of GP mediated delivery of Dox-MSN even at low concentrations. Following a 24 h concentration it is likely that the Dox-MSN particle aggregates or Dox released from Dox-MSN or Dox-MSN/GP will accumulate in cells to a significant concentration to have an effect on growth arrest.

Additionally, Dox-MSN was delivered with and without GPs to 3T3 cells, which do not express glucan receptors. Following particle uptake for 3 h the DMEM medium was replaced in the wells to remove any GP or free MSN particles still not internalized by the cells. The cells were incubated for additional 48 hours and evaluated for Dox effect on cell growth. The results shown in Figure 32 indicate that Dox-MSN delivered using 25 k PEI-GP have an effect on growth arrest on 3T3-D1 cells, but not on 3T3 confirming

that GP mediated uptake is responsible for Dox delivery. In comparison, free MSN show

an effect on both 3T3 and 3T3-D1 cells.

4. Conclusion

This project led to the successful synthesis of seven different MSN samples. The MSN's capacity to bind to both doxorubicin and rifampicin were analyzed. It was concluded that the most successful method of binding MSNs and GPs was to attach phosphate functionalized MSNs to the outside of cationic PEI-GPs. This process had limitations in the level of Dox that was being bound. Dox-MSN-GP formulations show GP mediated delivery of Dox into 3T3- D1 cells causing growth arrest, but no cell death.

5. Future Work

The particles generated during the course of this project were designed to deliver Rifampicin (Rif) and Doxorubicin (Dox) to target cells. Through the background information and experimental data gathered during this project, technology can be further developed for more specific and efficient GP-MSN delivery systems.

The synthesis of MSN can be changed in the future to create a particle with a higher binding affinity for the target drugs Rif or Dox. Further changes in MSN synthesis can also be used to create samples for pH (i.e. polyacrylic acid modified MSN), thermosensitive (i.e. poly(N-isopropylacrylamide) modified MSN) or redox (i.e. cystamine modified MSN) controlled release of drugs.

Changes in MSN synthesis can also be used to generate more uniform MSN particles. By controlling the size of the particles being created, particles smaller than ~40nm can be generated that would be able to be trapped within the GPs, rather than just binding on the surface. This would allow for more drugs to be encapsulated per GP.

The last technique that can be developed from our work is specifically used for the delivery of Dox to tumor sites. By adding a magnetic binding capacity Dox would be security locked inside of the MSN. Once the macrophage cells uptake the GP-MSNs they retain them for a long period of time. Throughout the process, macrophages migrate into tumors and multiply. Once enough of the macrophage cells loaded with GP-MSNs have entered the tumors, the released drug will inhibit cell growth and eventually kill the cells.

In the case of this project, the goal was to load cells with Doxorubicin which, when

enough Dox was delivered to the macrophage cells, would eventually kill the 3T3-D1

cells. The drug would be released by adding a microwave directly over the site of the

tumor. This wavelength would cause degradation of the MSN and the release of the drug

in the target area. GP-MSNs have cell receptors that attract macrophage cells.

References

Aouadi, M., Tesz, G. J., Nicoloro, S. M., Wang, M., Chouinard, M., Soto, E., et al. (2009). Orally Delivered siRNA Targeting Macrophage MAP4K4 Supresses Systemic Inflammation. *Nature , 458*, 1180-1184.

Aubel-Sadron, G., & Londos-Gagliardi, D. (1984). Danorubicin And Doxorubicin, Anthracycline Antiobiotics, A Physicochemical And Biological Review. *Biochimie , 66*, 333-352.

Bonadonna, G., Monfardini, S., De Lena, M., Fossati-Bellani, F., & Beretta, G. (1970). Phase I and preliminary phase II evaluation of adriamycin (NSC 123127). *Cancer Research , 30* (10), 2572-2582.

Brown, G D; Gordon, S;. (2001). Immune recognition: a new receptor for beta-glucans. *Nature* (413), 36-7.

Carter, C., Gaspar, A., & Leise, J. (1955). Resazurin staining of bacterial colonies on membrane filters. *The Journal of Bacteriology , 70* (5), 623.

Gillies, E. R., & Frechet, J. M. (2005). pH-Responsive Copolymer Assemblies for Controlled Release of Doxorubicin. *Bioconjugate Chemistry , 16*, 361-368.

Hong, F., Yan, J., Baran, J. T., Allendorg, D. J., Hansen, R. D., Ostroff, G. R., et al. (2004). Mechanism By Which Orally Administered b-1,3-Glucans Enhance the Tmoricidal Acvtivity of Antitumor Monoclonal Antibodies in Murine Tumor Models. *Journal of Immunology , 173*, 797-806.

Huang, H., Ostroff, G. R., Lee, C. K., Wang, J. P., Specht, C. A., & Levitz, S. M. (2009). Distinct Patterns Of Dendritic Cell Cytokine Release Stimulated By Fungal b-glucans and Toll-like Receptor Agonists. *Infection and Immunity , 77*, 1774-1781.

Huang, H; Ostroff, G; Lee, C; Specht, C; Levitc, S; Wang, J;. (2009). Distinct patterns of dendritic cell cytokine release stimulated by fungal beta-glucans and toll-like receptor agonists. *Infection And Immunology , 77* (5), 1774-81.

Huh, S., Wiench, J., Yoo, J., Pruski, M., & Lin, V. (2003). Organic functionalization and morphology control of mesoporous silica via a co-condensation synthesis method. *Chemistry of Materials* , 4247-4256.

Kresge, C. T., Leonowicz, M. E., Roth, W. J., Vartuli, J. C., & Beck, J. S. (1992). Ordered Mesoporous Molecular Sieves Synthesized By A Liquid Crystal Template Mechanism. *Nature , 359*, 710-712.

Lu, J., Liong, M., Sherman, S., Xia, T., Kovochich, M., & Nel, A. E. (2007). Mesoporous Silica Nanoparticles for Cancer Therapy: Energy-Dependent Cellular Uptake and Delivery of Paclitaxel to Cancer Cells. *Nano Biotechnology* , 89-95.

Lu, J., Liong, M., Zink, J. I., & Tamanio, F. (2007). Mesoporous Silica Nanoparticles as a Delivery System for Hydrophobic Anticancer Drugs. *Small* , 1341-1346.

Meng, H., Liong, M., Xia, T., Li, Z., Ji, Z., Zink, J. I., et al. (2010). Engineered Desing of Mesoporous Silica Nanoparticles to Deliver Doxorubicin and P-Glycoprotein siRNA To Overcome Drug Resistance In A Cancer Cell Line. *ACSNano , 4* (8), 4539-4550.

Niraula, N. P., Kim, S.-H., Sohng, J. K., & Kim, E.-S. Biotechnological doxorubicin production: pathway and regulation engineering of strains for enhanced production. *Applied Microbiology and Biotechnology , 87* (4), 1187-1194.

Sajbidor, J., & Gergoa, J. (1994). Lipid Analysis of Baker's Yeast . *Journal of Chromatography* , 191-195.

Sensi, P., Margalith, P., & Timbal, M. (1959). Rifomycin, a new antibiotic; preliminary report. *II Farmaco , 14* (2), 146-147.

Soto, E. R., Kim, Y. S., Lee, J., Kornfield, H., & Ostroff, G. (2010). Glucan Particles

Encapsulated Rifampicin for Targeted Delivery to Macrophages. *Polymers , 2*, 681-689.

Soto, E., & Ostroff, G. (2010). *Patent No. 61/373828.* U.S.

Soto, E., & Ostroff, G. (2007). Oral Macrophage Mediated Gene Delivery System. *NSTI*

Nanotech Technical Proceedings , 2, 378-381.

Soto, E., & Ostroff, G. R. (2008). Characterization of Multilayered Nanoparticles Inside

Yeast Cell Wall Particles for DNA Delivery. *Bioconjugate Chemistry , 19*, 840-848.

Soto, E., & Ostroff, G. (2011). Use of beta-1,3-D-glucans for Drug Delivery

Applications. *In press* .

Soto, E., & Ostroff, G. (2011). Use of beta-Glucans for Drug Delivery Applications. In

V. Vetvicka, & M. Novak (Eds.), *Biology and Chemistry of Beta Glucan* (Vol. 1).

Bentham Press.

Soto, E., Kim, Y. S., Lee, J., Kornfield, H., & Ostroff, G. (2010). Glucan Particle

Encapsulated Rifampicin for Targeted Delivery to Macrophages. *Polymers , 2*, 681-689.

Soto, E.R., Ostroff, G. (2008). Characterization of Multilayered Nanoparticles

Encapsulated in Yeast Cell Wall Particles for DNA Delivery. *Bioconjugate Chem.* , 840-

848.

Tesz, G; Aouadi, M; Prot, M; Nicoloro, S; Boutet, E; Amano, S; Goller, A; Wang, M;

Guo, C; Salomon, W; Virbasius, J; Baum, R; O'Connor Jr., M; Soto, E; Ostroff, G;

Czech, M;. (2011). Glucan Particles for Selective Delivery of siRNA to Phagocytic Cells

in Mice. *Biochemical Journal , in press*.

Trewyn, B. G., Slowing, I., Giri, S., Chen, G. T., & Lin, V. S. (2007). Synthesis and

Functionalization of Mesoporous Silica Nanoparticle Based on the Sol-Gel Process and

Applications in Controlled Release. *Accounts of Chemical Research , 40* (9), 846-853.

Tupin, A., Gualtieri, M., Roquet-Baneres, F., Morichaud, Z., Brodolin, K., & Leonetti, J. (2010). Resistance to Rifampicin: At The Crossroads Between Ecological, Genomic, and medical Concerns. *International Journal of Antimicrobial Agents , 35*, 519-523.

Young, S; Ostroff, G; Patti, C; Erdley, R; Roberts, J; Anonini, J; Castranova, V;. (2007). A Comparison of the Pulmonary Inflammatory Potential of Different Components. *Journal of Toxicology and Environmental Health Part A* , 116-1124.

Zhang, Y., Zhi, Z., Jiang, T., Zhang, J., Wang, Z., & Wang, S. (2010). Spherical mesoporous silica nanoparticles for loading and release of hte poorly water-soluble drug telmisartan. *Journal of Controlled Release , 145* (3), 257-263.

Appendix: Figures
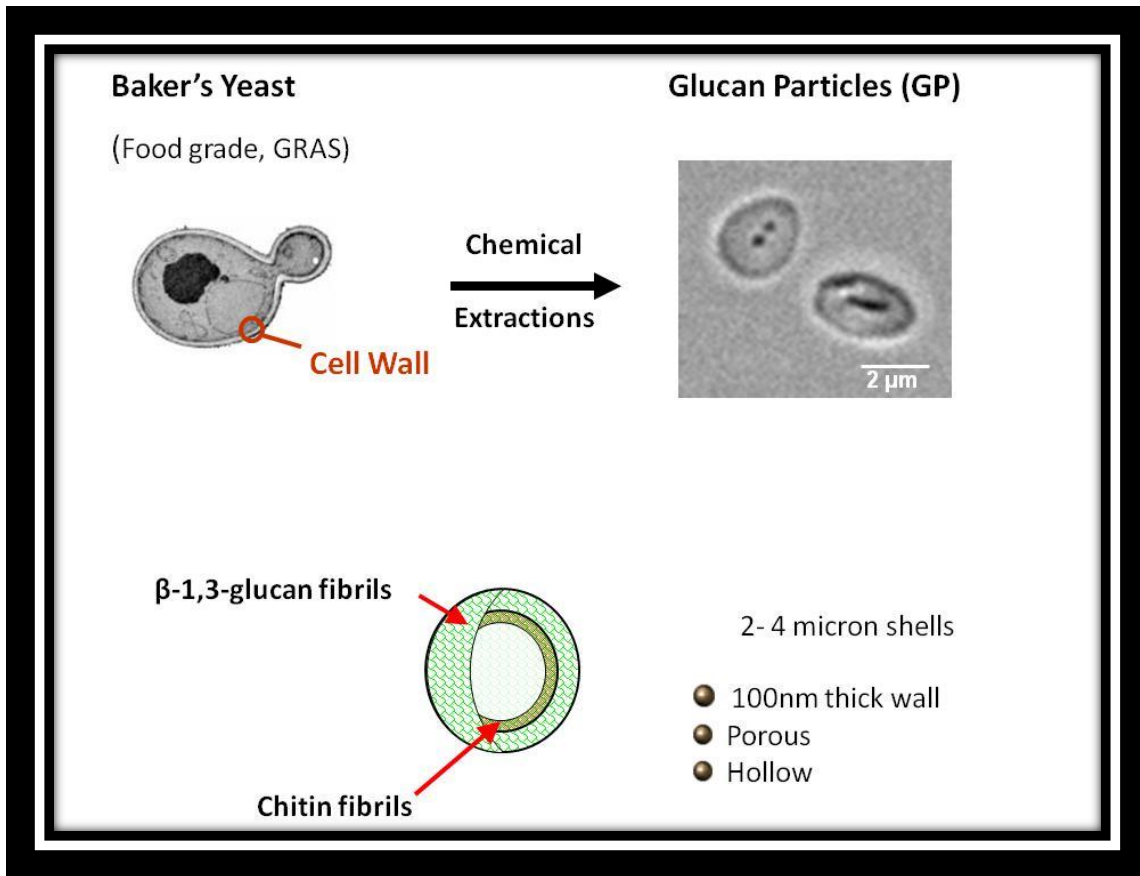
FIGURE 1: TRANSMISSION ELECTRON MICROSCOPE (TEM) IMAGES OF BAKER'S YEAST AND HOLLOW GLUCAN PARTICLES. SCHEMATIC REPRESENTATION OF A GP.

Figure 1 illustrates the process of chemically treating Baker's Yeast cells in order to achieve the hollow, porous glucan particles (GPs). The chemical composition is also indicated.
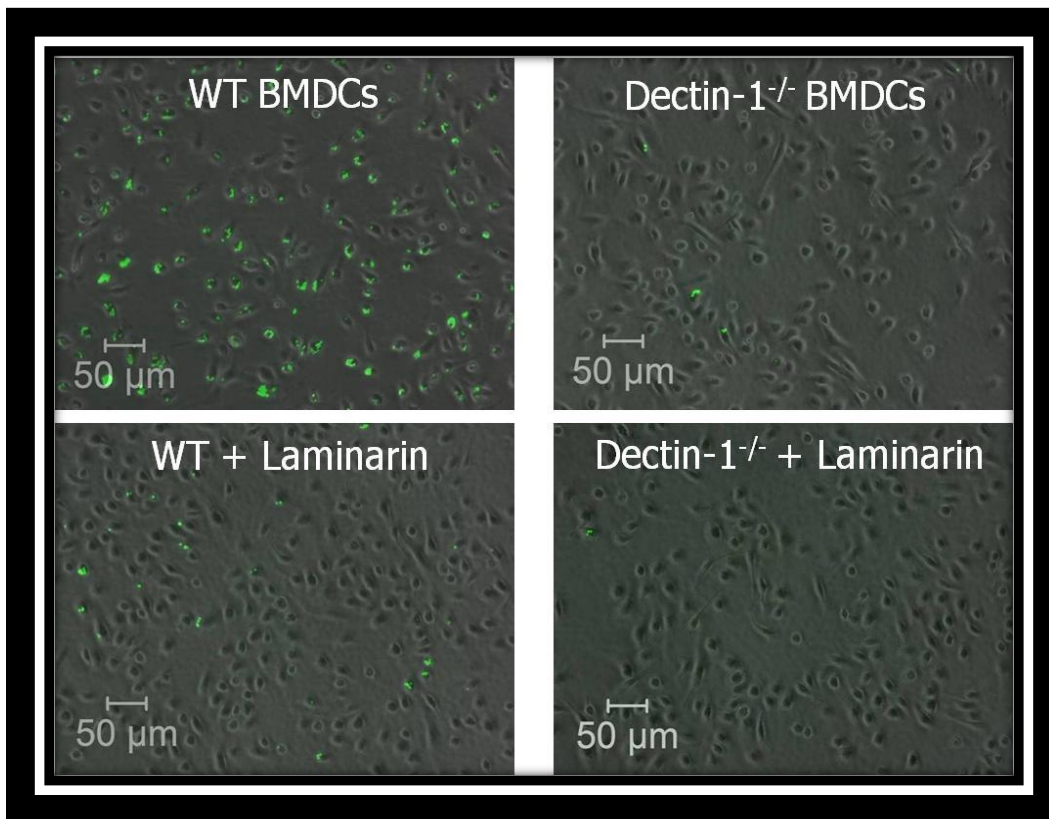
FIGURE 2: DECTIN-1 MEDIATED RECEPTOR UPTAKE OF FLUORESCENTLY LABELED GLUCAN PARTICLES BY BONE MARROW DENDRITIC CELLS (BMDC). CELLS FROM A WILD TYPE (WT) MOUSE EFFICIENTLY PHAGOCYTOSE GPS. THE D1 KNOCK OUT BMDCS DO NOT SHOW PARTICLE UPTAKE. ADDITION OF A SOLUBLE B-GLUCAN, LAMINARIN, INHIBITS GP UPTAKE (HUANG H. , OSTROFF, LEE, SPECHT, LEVITC, & WANG, 2009).

Figure 2 shows fluorescent microscope images superimposed over bright field images. The wild type Bone Marrow Dendritic Cells (WT BMDCs) show uptake of the fluorescent glucan particles while the BMDC with the glucan receptor (D1) knocked out did not show uptake. Wild type mouse cells also showed glucan uptake, but no uptake in the D1 knockout cells.
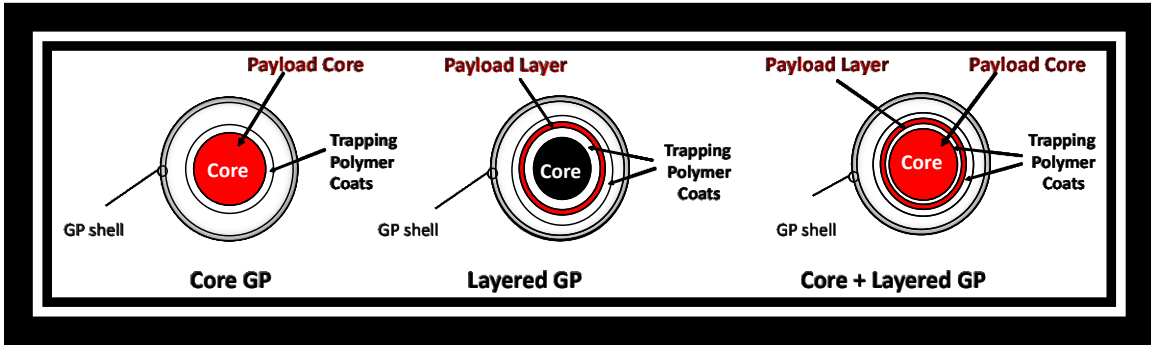
FIGURE 3: GP FORMULATIONS SHOWING POSSIBLE LOCATIONS OF PAYLOAD MACROMOLECULES USING POLYPLEX CORE SYNTHESIS AND LAYER-BY-LAYER (LBL) ELECTROSTATIC ASSEMBLY

Figure 3 illustrates the different compositions of glucan particles.
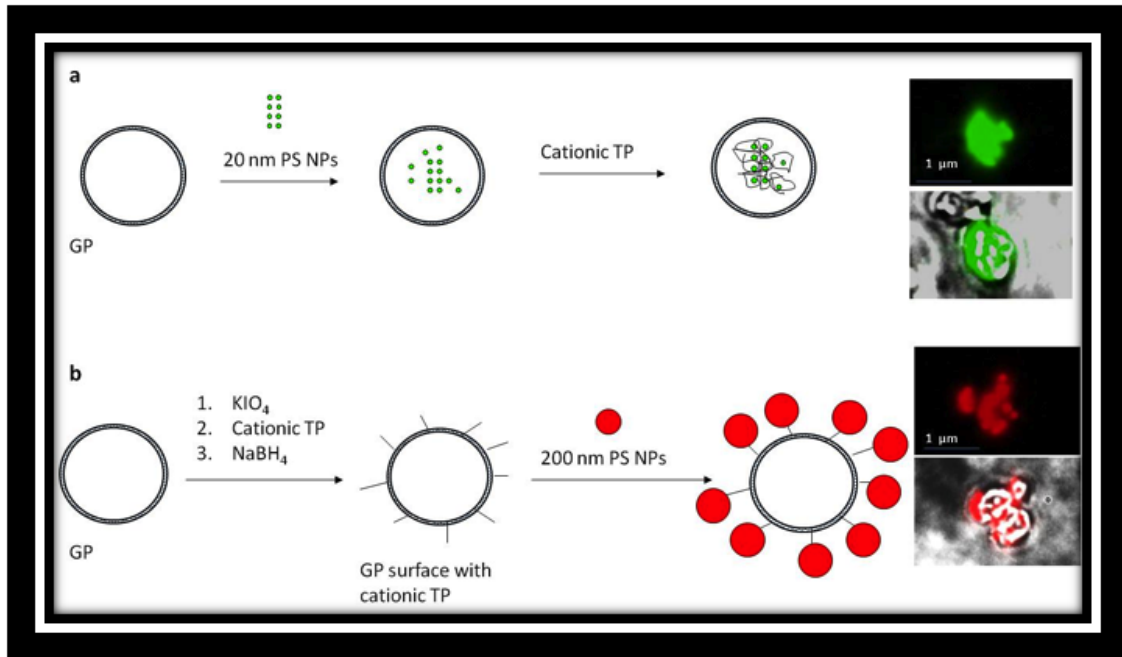
FIGURE 4: SCHEMATIC REPRESENTATION OF PREFORMED CARBOXYLATED POLYSTYRENE NANOPARTICLE LOADING: (A) INSIDE GPS, (B) ON THE SURFACE OF A CATIONIC GP. (20NM NPS ARE SHOWN IN GREEN CIRCLES AND 200NM NPS IN RED CIRCLES) (SOTO & OSTROFF, ENCAPSULATION OF NANOPARTICLES INSIDE YEAST CELL WALL PARTICLES FOR RECEPTOR-TARGETED DRUG DELIVERY, 2010)

Figure 4 shows two possibilities for binding nanoparticles and glucan particles. The first possibility is loading the nanoparticles into the glucan particle and the second option is loading the nanoparticles on the outside of the glucan particles. Microscopic images are also shown of this process.
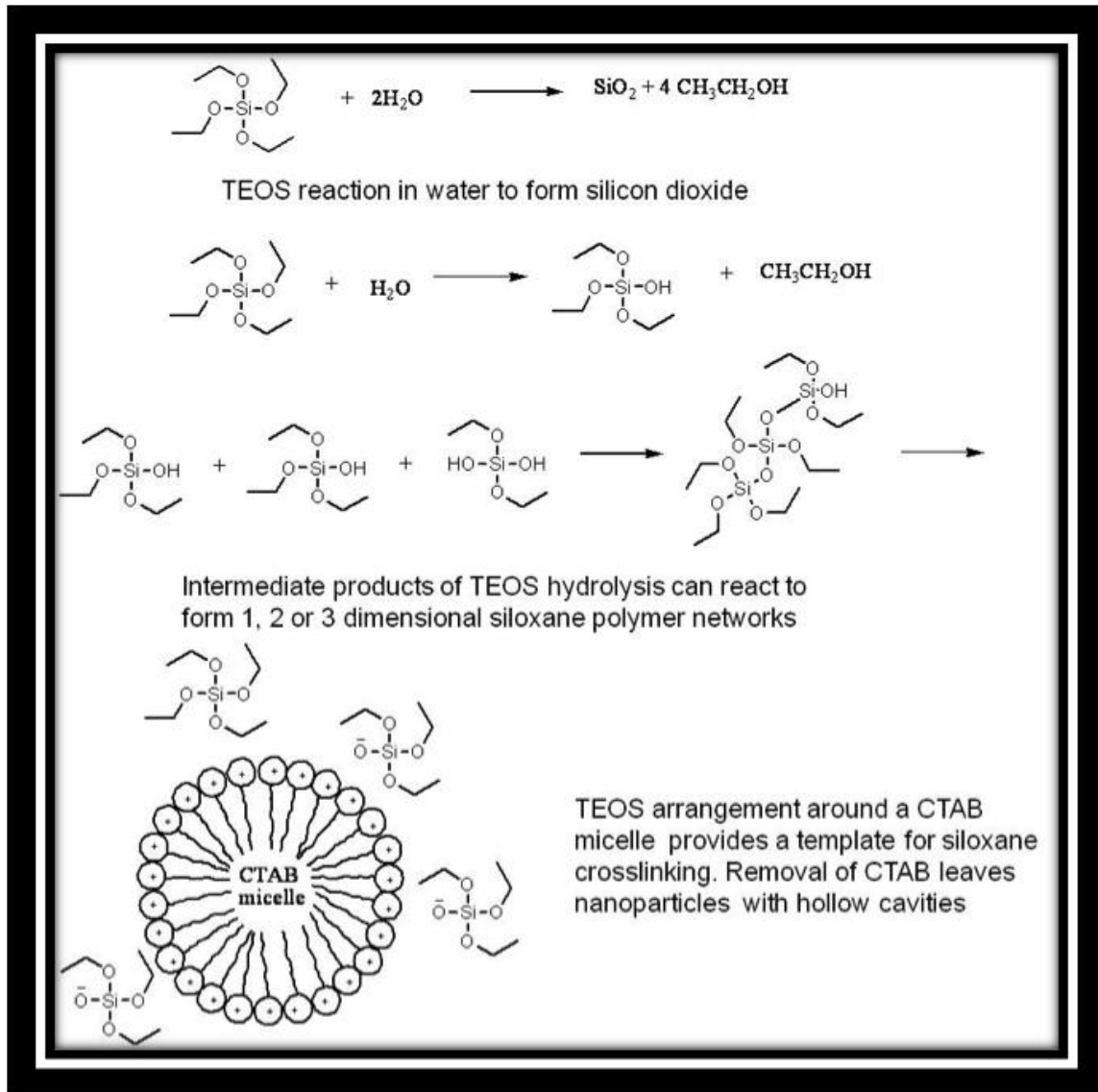
FIGURE 5: SCHEMATIC REPRESENTATION OF MSN SYNTHESIS USING TETRAETHYL ORTHOSILICATE (TEOS)

Figure 5 shows the process of synthesizing MSN. A CTAB micelle is shown as a template with the orthosilicates arranging themselves around the micelle in a spherical orientation.
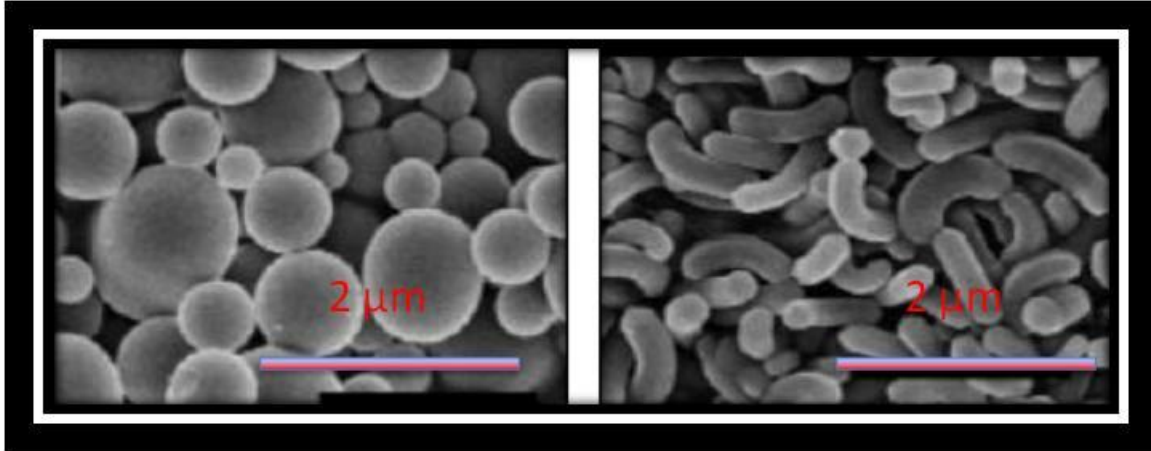
FIGURE 6: FIELD EMISSION SCANNING ELECTRON MICROSCOPY (FESEM) IMAGES OF NANO-ROD (LEFT) AND NANO-SPHERICAL (RIGHT) MSNS (HUH, WIENCH, YOO, PRUSKI, & LIN, 2003).

Figure 6 shows microscopic images of the two possible MSN structures. The first is the spherical shape which was used for this project; the other is a rod composition.
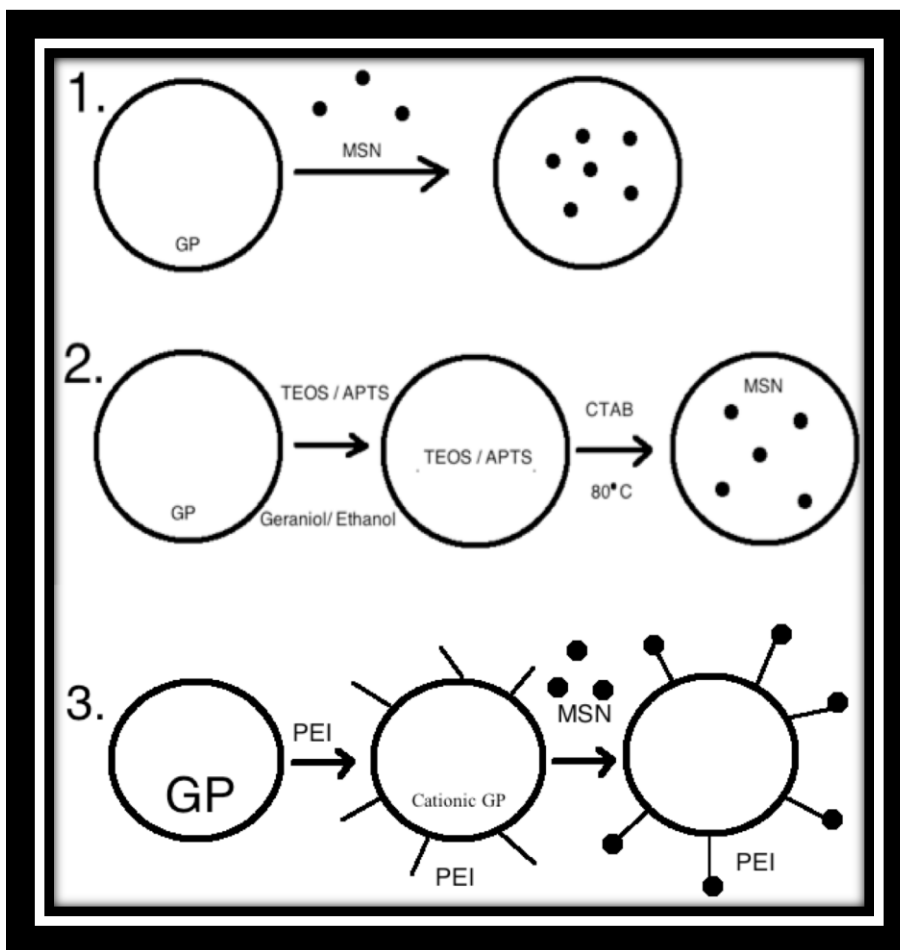
FIGURE 7: SCHEMATIC REPRESENTATION OF THREE STRATEGIES TO INCORPORATE MSN INTO GLUCAN PARTICLES: (1) ABSORPTION OF MSN <40NM THROUGH THE GLUCAN PARTICLE PORES, (2) LOADING OF MSN REAGENTS FOR *IN SITU* SYNTHESIS OF NANOPARTICLES, (3) ELECTROSTATIC BINDING OF ANIONIC MSNS TO CATIONIC GPS.

Figure 7 shows the three different strategies taken for this project to create GP/MSN complexes. The first process includes putting preformed MSNs inside the GPs. The second process would involve synthesizing the MSNs inside of the GPs. The third process would involve functionalizing the outside of the GPs and attaching the MSNs to the surface of the GPs.
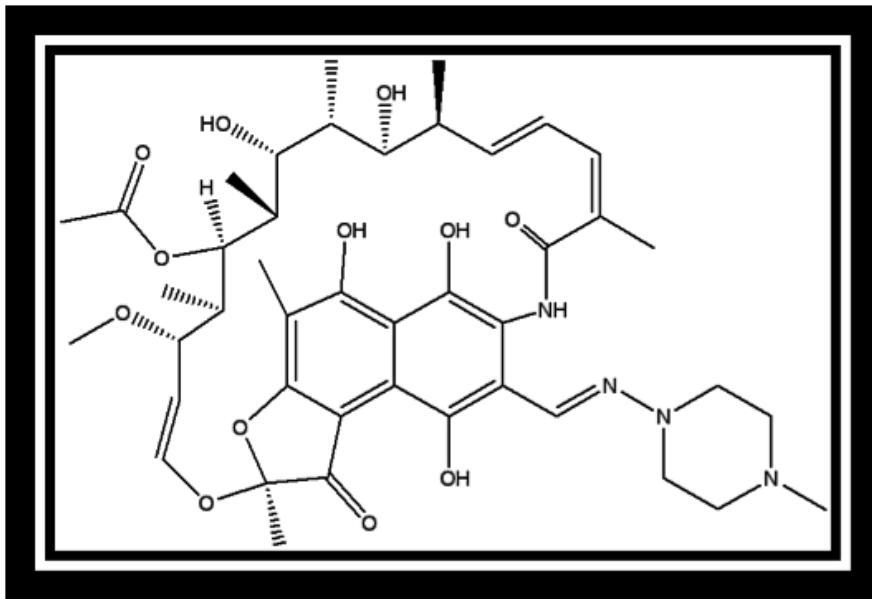
FIGURE 8: THE CHEMICAL STRUCTURE OF RIFAMPICIN

Figure 8 shows the chemical structure of the Tuberculosis drug Rifampicin (Rif).
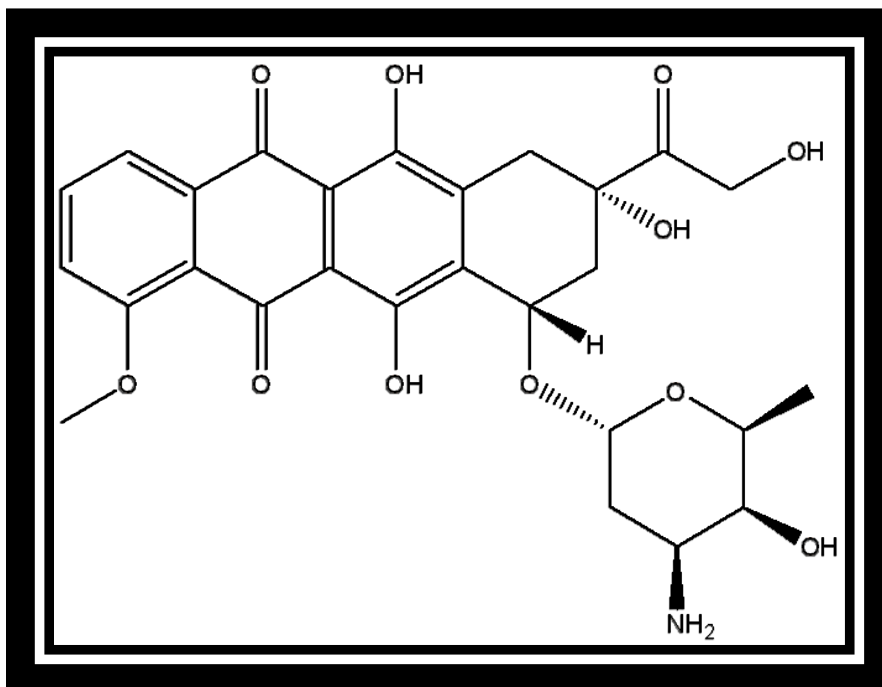
FIGURE 9: THE CHEMICAL STRUCTURE OF DOXORUBICIN

Figure 9 shows the chemical structure of the cancer drug Doxorubicin (Dox).

Table 1 shows the composition of each of the MSN samples.

MSN	MSN Composition	APTS	f-APTS	TEOS	PO4
MSN-1	TEOS	-	-	2.5 mL	-
MSN-2	TEOS/PO4	-	-	2.5 mL	0.63 mL
MSN-3	TEOS/APTS	12 µL	-	2.5 mL	-
MSN-4	TEOS/f-APTS	-	0.3 mL	2.5 mL	-
MSN-5	TEOS/f-APTS/PO4	-	0.3 mL	2.5 mL	0.63 mL
MSN-6	TEOS/APTS/PO4	12 µL	-	2.5 mL	0.63 mL
MSN-7	TEOS Control	-	-	2.5 mL	-

TABLE 1: COMPOSITION OF MSN SAMPLES

Table 2 shows the conditions necessary to create cationic glucan particles.

GP sample	Polymer	% TP	mL TP	mL Water
25 kPEI-GP	25 k polyethylenimine	10	4.2	7.8
CN-GP	Chitosan	2	7.9	4.1
PLL-GP	Poly-L-lysine	0.1	10.5	1.5

TABLE 2 REACTION CONDITIONS TO PRODUCE CATIONIC GLUCAN PARTICLES (15 MG SCALE).

Table 3 shows the loading solvent mixtures that were used when attempting to synthesize MSN within the GPs.

Tube	TEOS (T)	DMSO (D)	F-APTS	Geraniol (G)
TG	90 μL	-	10 μL	9 μL
TDG	90 μL	10 μL	10 μL	9 μL
TD10%	90 μL	11 μL	10 μL	-
TD50%	90 μL	100 μL	10 μL	-

TABLE 3: LOADING SOLVENT MIXTURES EVALUATED FOR *IN SITU* SYNTHESIS OF MSN.

Figure 4 shows the optimal loading solvent concentrations.

	μL TEOS	μL APTS	μL EtOH	μL Geraniol
A	900	0	90	100
B	900	10	90	90

TABLE 4: OPTIMAL LOADING SOLVENT MIXTURES FOR *IN SITU* SYNTHESIS OF MSN.
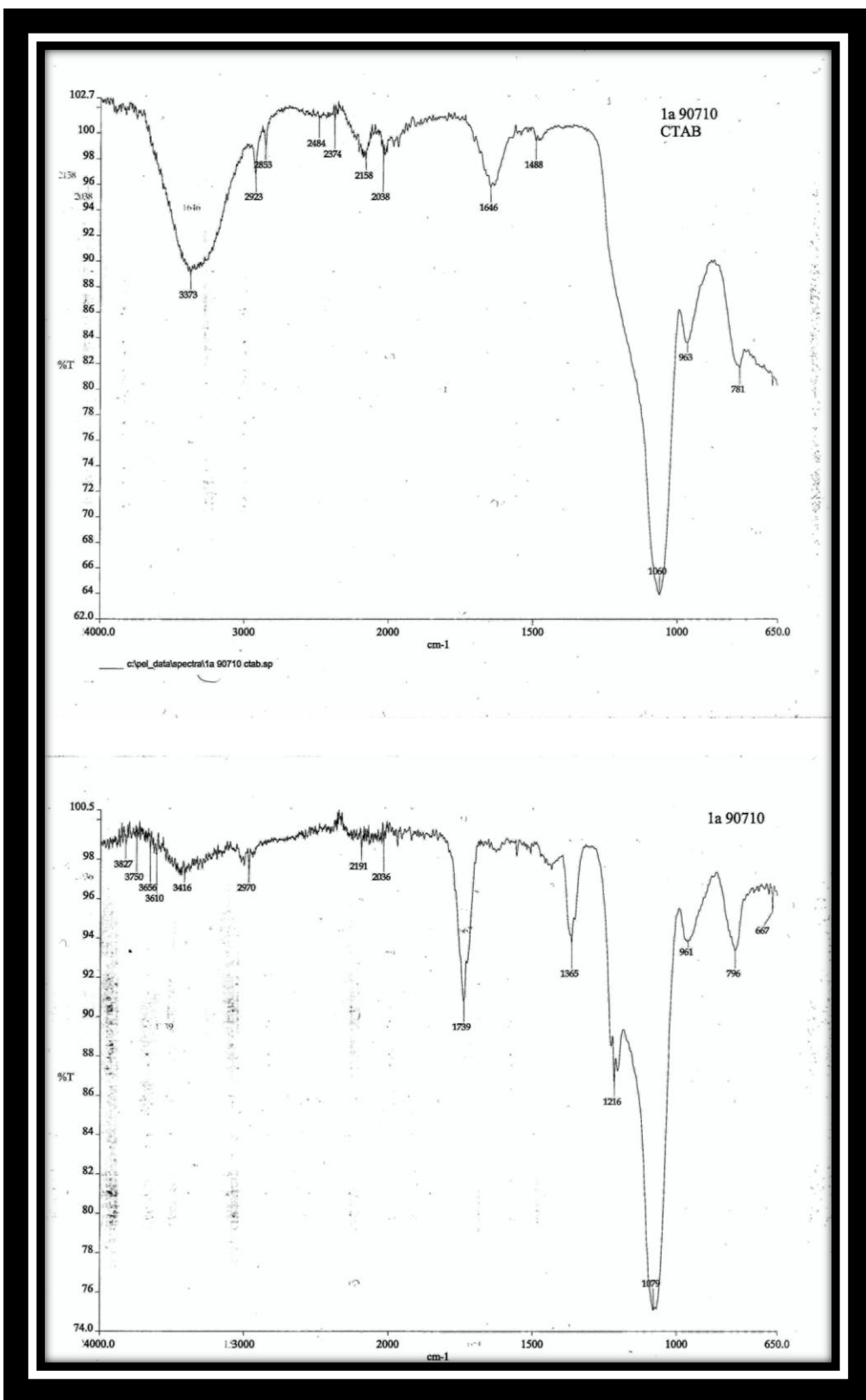
FIGURE 10: IR SPECTRUM OF MSN1 BEFORE (TOP) AND AFTER (BOTTOM) CTAB EXTRACTION

Figure 10 includes the IR spectra for MSN1 before and after the CTAB micelle extraction. The upper figure shows a broad band at 3373 indicating the presence of CTAB; this band is not present in the lower figure.
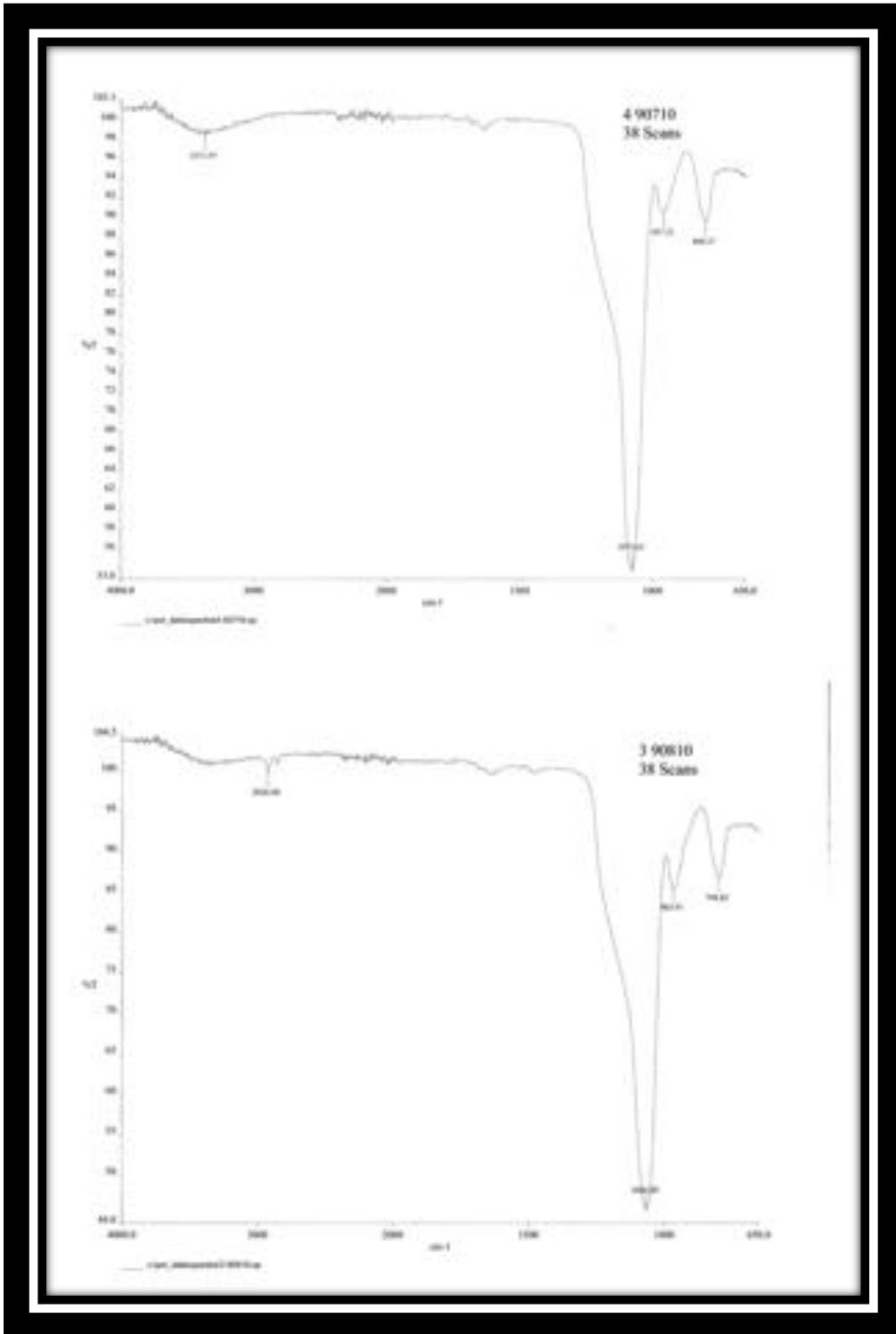
FIGURE 11: IR SPECTRA OF MSN-3 (TOP) AND MSN-6 (BOTTOM)

Figure 11 shows the IR spectra for samples MSN-3 and MSN-6 indicating the presence of different functional groups.

Table 5 includes the zeta potential and DLS size measures for all MSN samples.

MSN	MSN Composition	Zeta Potential results	DLS results	
		Zeta Potential (mV)	Size (nm)	PDI
MSN-1	TEOS	-2.94 (100%)	120	1
MSN-2	TEOS/APTS	15.7 (100%)	129	0.867
MSN-2a	TEOS/fAPTS	-3.8 (100%)	214	1
MSN-3a	TEOS/fAPTS/PO4*	-33 (95%), -16.5 (5%)	101, 719	0.65
MSN-3	TEOS/APTS/PO4	-31.1 (96.3%), -10.4 (3.7%)	119, 351	0.424
MSN-4	TEOS/PO4	-26.4 (100%)	72	1
MSN-5	TEOS control	-4.8 (100%)	638	0.806
		% intensity in parenthesis		

TABLE 5: ZETA POTENTIAL AND DLS SIZE MEASUREMENTS OF MSN SAMPLES
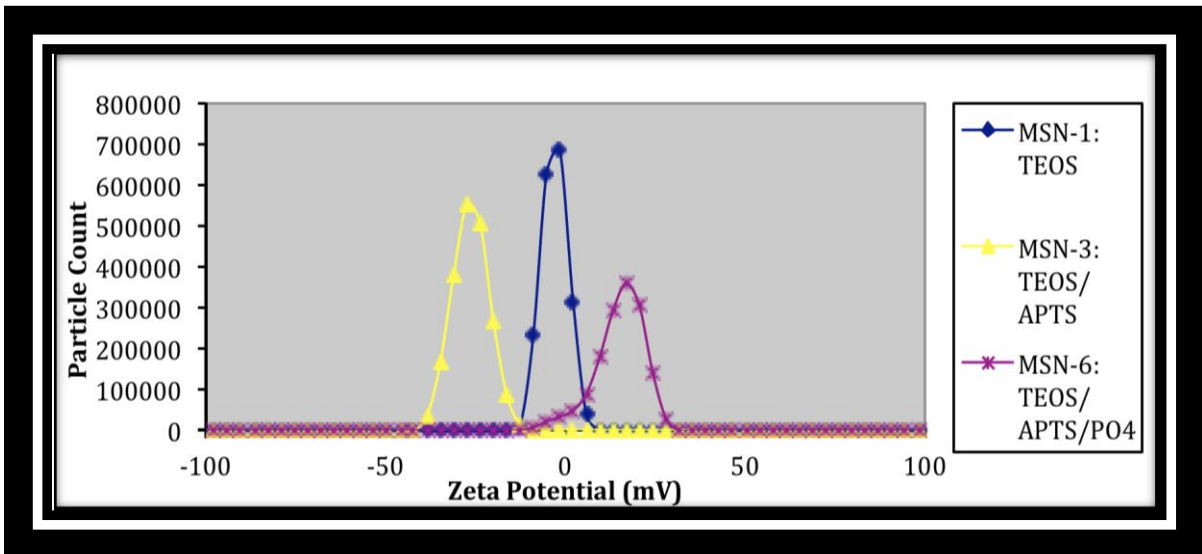
FIGURE 12: ZETA POTENTIAL OF MSN SAMPLES

Figure 12 graphically illustrates the data presented in table 5; particle count is graphed versus zeta potential for samples MNS-1, MSN-3, and MSN-6.This graph indicates the difference in zeta potential depending on the different functional groups.
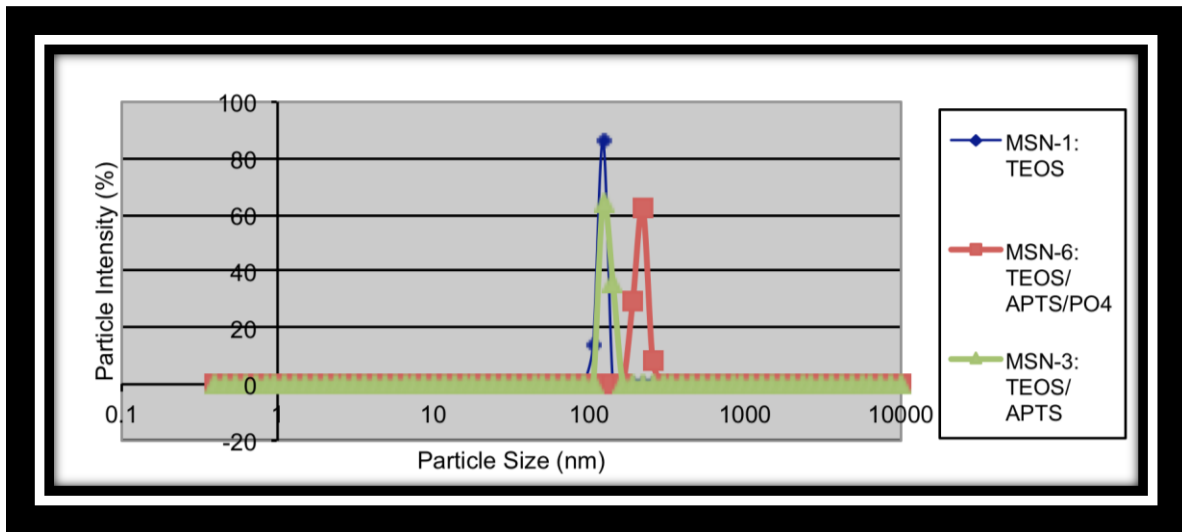
FIGURE 13: PARTICLE SIZE OF MSN SAMPLES

Figure 13 shows the particle size of three different MSN samples versus the intensity of the particles.
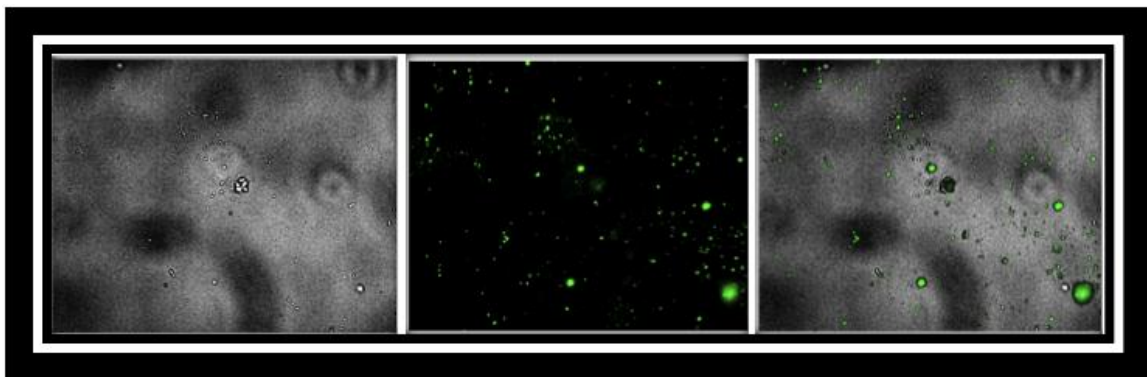
FIGURE 14: 20X MICROSCOPIC IMAGES OF MSN PREPARED WITH TEOS AND F-APTS

Figure 14 shows the brightfield image of the MSNs prepared with TEOS and F-APTS, the fluorescent image of fluorescent MSNs, and an overlay of the two images. This image is used to show the successful synthesis of fluorescent MSN.
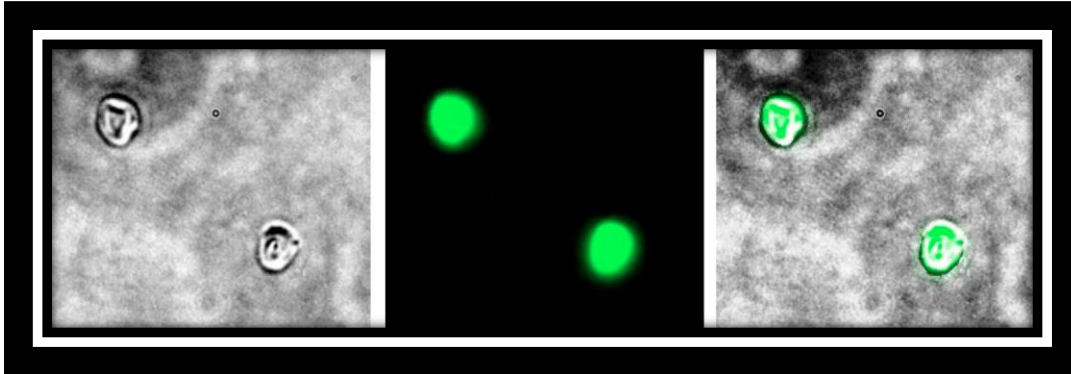
FIGURE 15: F-MSN (TEOS/F-APTS) SYNTHESIS INSIDE GLP

Figure 15 shows the brightfield image of the GLPs, the fluorescent image of fluorescent MSNs, and an overlay of the two images. In the overlaid image is it possible to see that MSN samples were synthesized with in the GLPs.
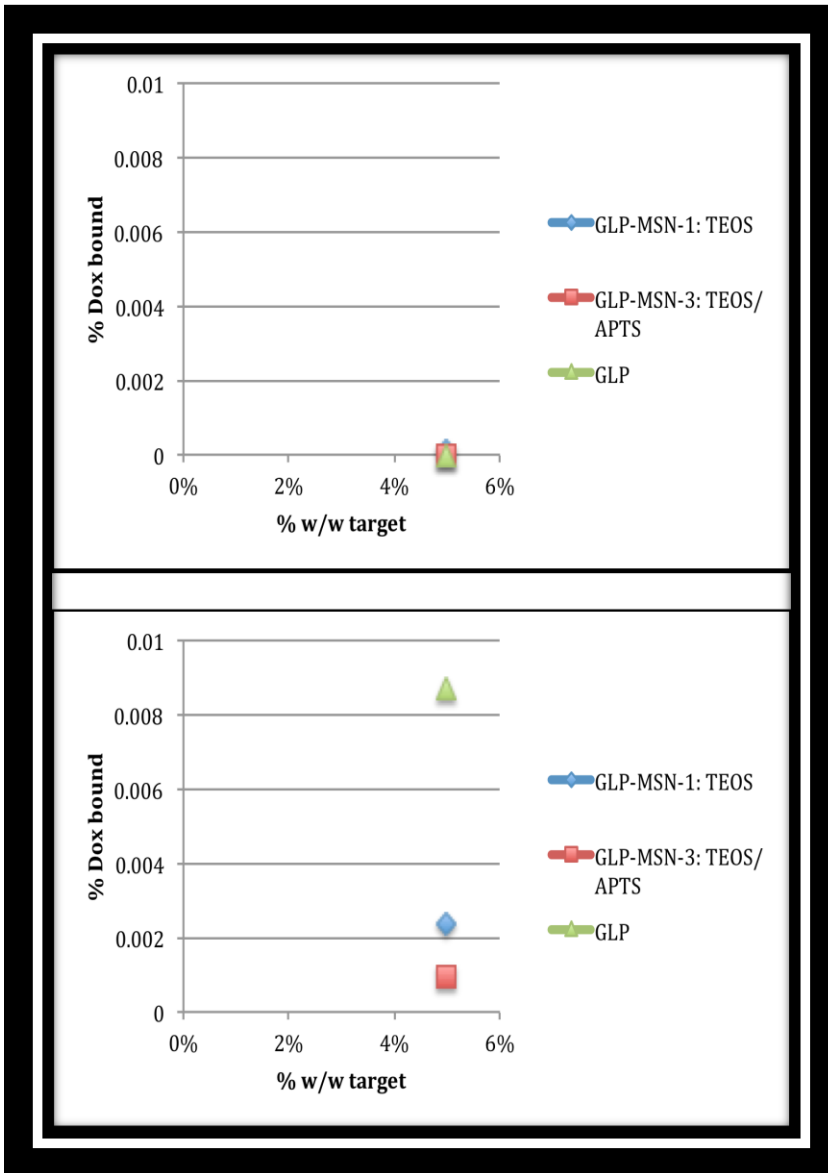
FIGURE 16 : PERCENT OF DOX BOUND INSIDE OF DIFFERENT GP-MSN SAMPLES LOADED IN WATER (TOP) AND 50% DMSO (BOTTOM)

Figure 16 shows the amount of Dox bound to different GP-MSN samples. The top image shows loading in water, the amount of Dox bound is negligible due to MSNs tendency to shrink in water. The bottom image shows the samples loaded in 50% DMSO 50% water. The amount of Dox bound was more significant though it never reached over 0.01% Dox bound.
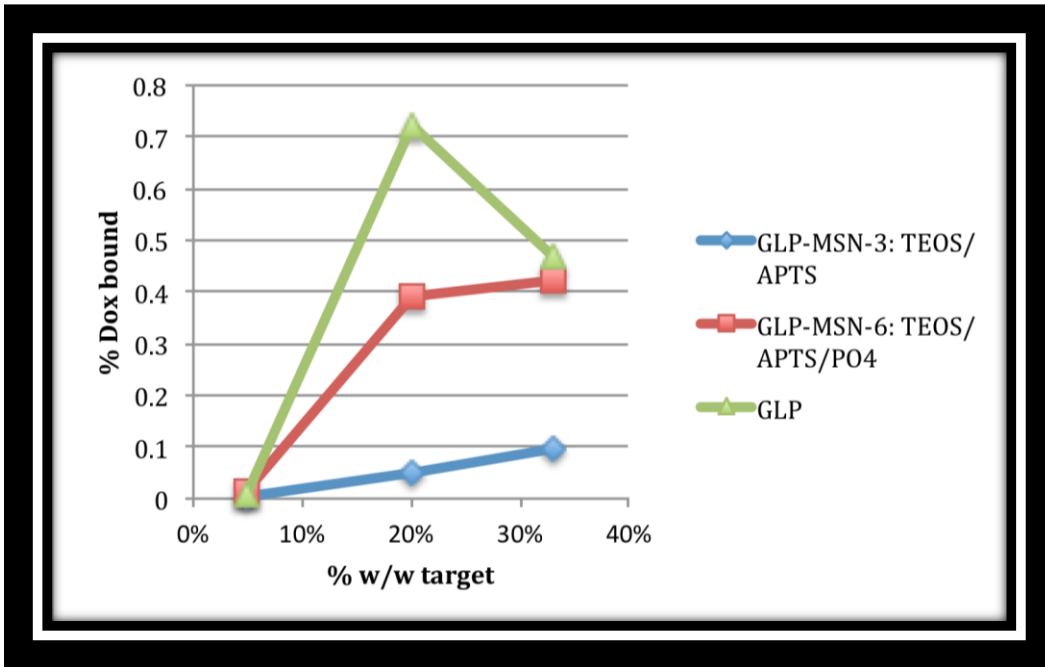
FIGURE 17: PERCENT OF DOX BOUND INSIDE OF DIFFERENT GLP-MSN SAMPLES WHEN LOADED IN 50% DMSO

Figure 17 shows the percent of Dox bound at different percent weight to weight targets for two samples of MSN and GLP controls. The GLP control showed the highest amount of Dox bound. These results indicate that this method was unsuccessful.
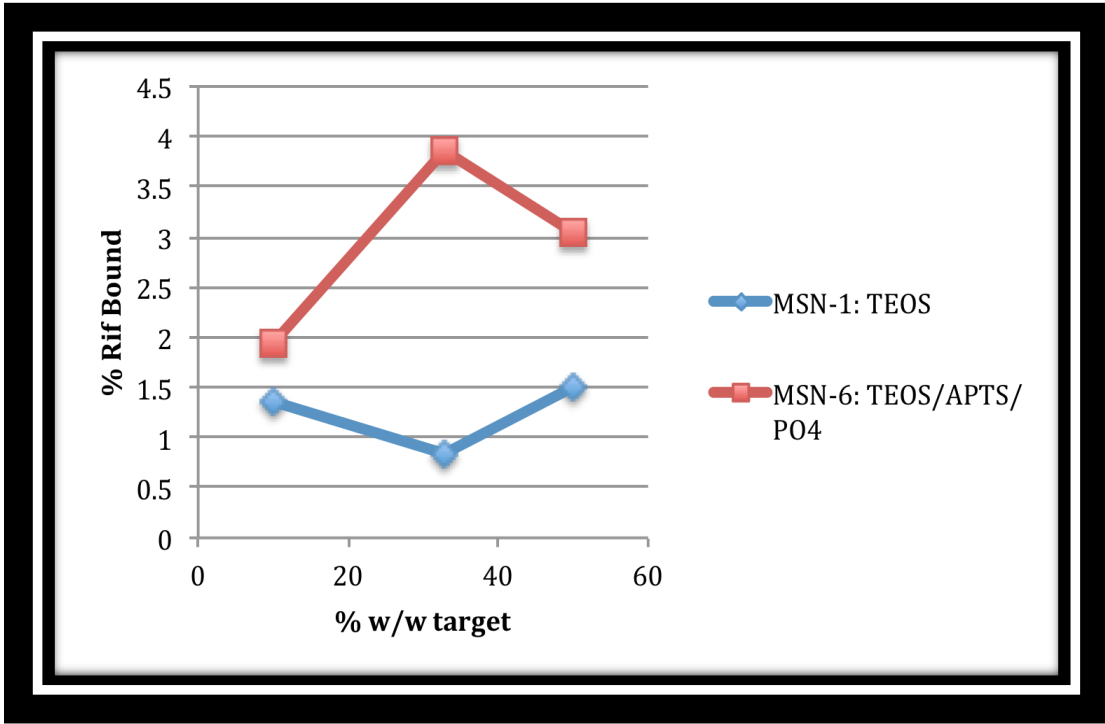
FIGURE 18: PERCENT OF RIF BOUND TO (A) MSN-1: TEOS AND (B) MSN-6: TEOS/APTS/PO4

Figure 18 shows the percentage of Rif that bound to a neutral MSN and an anionic MSN. The anionic MSN showed overall higher binding capacity.
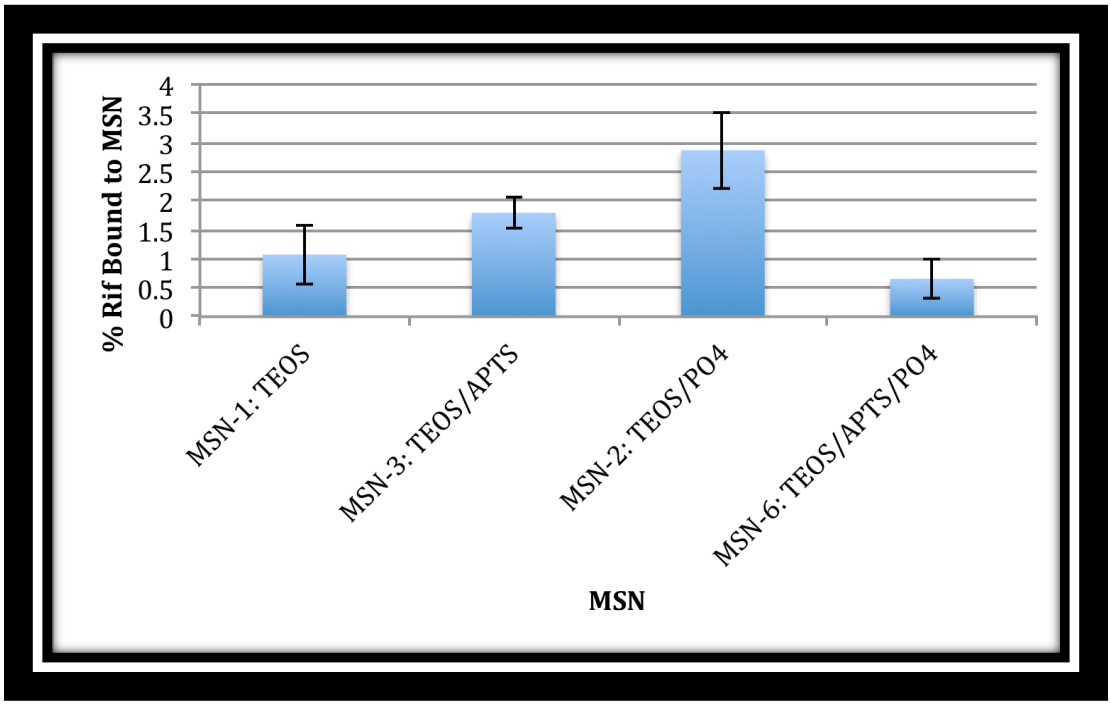
FIGURE 19: PERCENT OF RIF BOUND TO FOUR DIFFERENT MSN SAMPLES

Figure 19 shows the percent of Rif bound to 4 different MSN samples. The highest binding was seen in sample MSN-2.

Table 6 shows the concentrations of Rif-MSNs used during the MIC assay.

Rif-MSN (mg/mL)	Water Neg. ctrl. 100µL	Rif-MSN 1 100µL	Rif-MSN 2 100µL	Rif-MSN 3 100µL	Rif-MSN 4 100µL	MSN 5 100µL	Rif Stock Pos. ctrl. 0.4mg/mL 100µL
50	0.4978	0.5379	-0.2276	-0.0395	-0.1282	-0.3725	0.0107
25	0.5070	0.3755	-0.3028	-0.1494	-0.1651	-0.0573	0.0096
12.5	0.4395	0.4437	-0.2752	0.2093	-0.3626	-0.0109	0.0234
6.25	0.4563	0.3442	-0.1866	0.2432	0.0406	0.1060	0.0294
3.125	0.5031	0.4616	0.0265	0.2411	0.2638	0.1404	0.0203
1.565	0.4895	0.4468	0.2760	0.2651	0.2786	0.2116	0.3860
0.78	0.5683	0.4140	0.3215	0.2860	0.3414	0.2884	0.1210
0.39	0.5715	0.4493	0.4441	0.4100	0.4380	0.4172	0.5286

TABLE 6: RIF-MSN MIC ASSAY

FIGURE 20: MIC PLATES WITH COLUMNS IN REFERENCE TO TABLE 6

Figure 20 shows the MIC plate. The samples added to each well are indicated in Table 6. In this assay cell death is indicated by blue wells while live cells are indicated by pink wells. Column 7 was used as a control to show the capacity for Rif to kill *E. coli* cells. The best results were seen from MSN-3-Rif and MSN-2-Rif.

FIGURE 21: PERCENT OF DOX BOUND TO (A) MSN-1 AND (B) MSN-6

Figure 21 shows the percent of Dox bound to sample MSN-1` and MSN-6. The anionic MSN-6 had much higher binding with the Dox compared to the MSN-1.
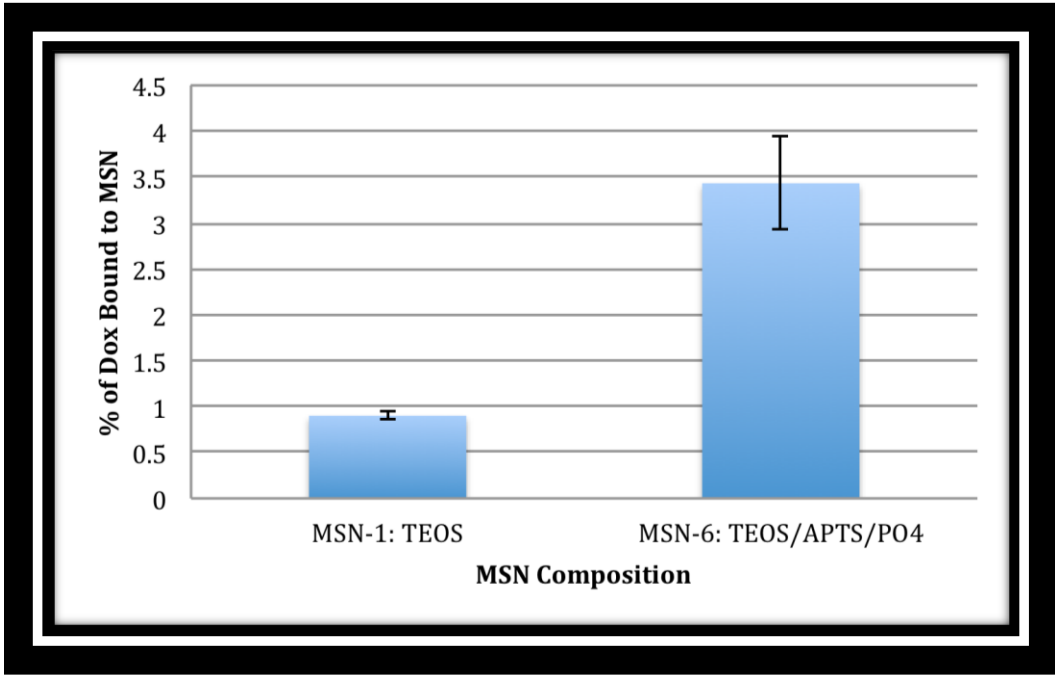
FIGURE 22: THE PERCENT OF DOX BOUND TO (A) MSN-1 AND (B) MSN-6

Figure 22 shows the percent of Dox bound to sample MSN-1` and MSN-6. The anionic MSN-6 had much higher binding with the Dox compared to the MSN-1.
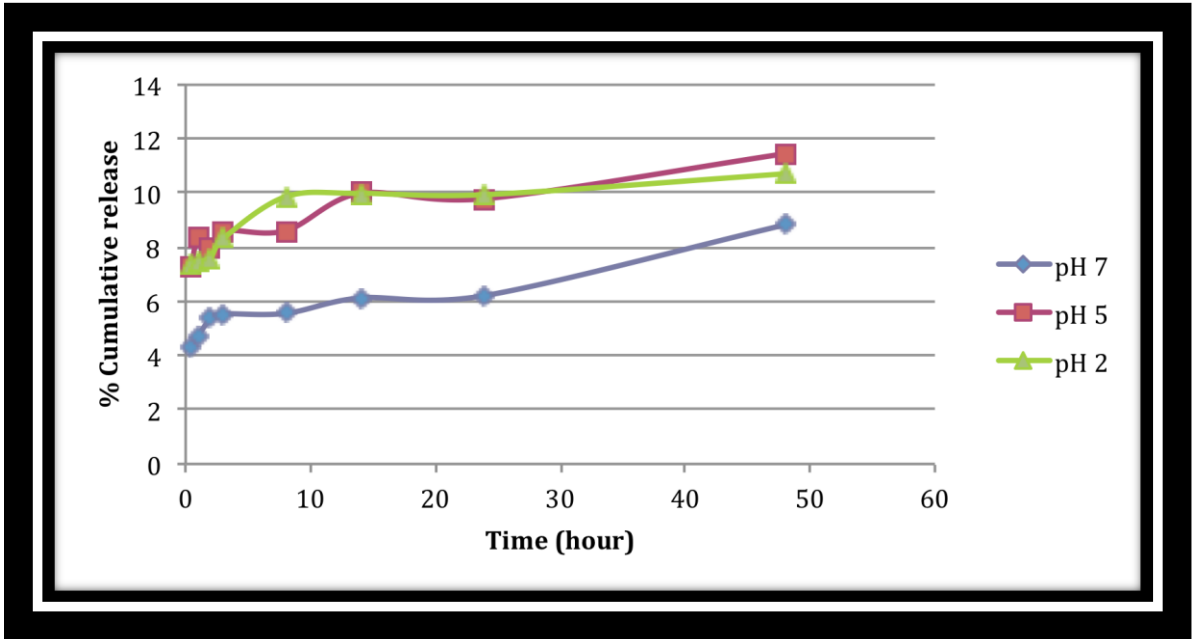
FIGURE 23: THE EFFECT OF pH ON DOX RELEASE FROM MSN-6.

Figure 23 shows the effect of pH on Dox release over time. The samples are most stable at pH 7 and show faster release at pH 5 and 2.
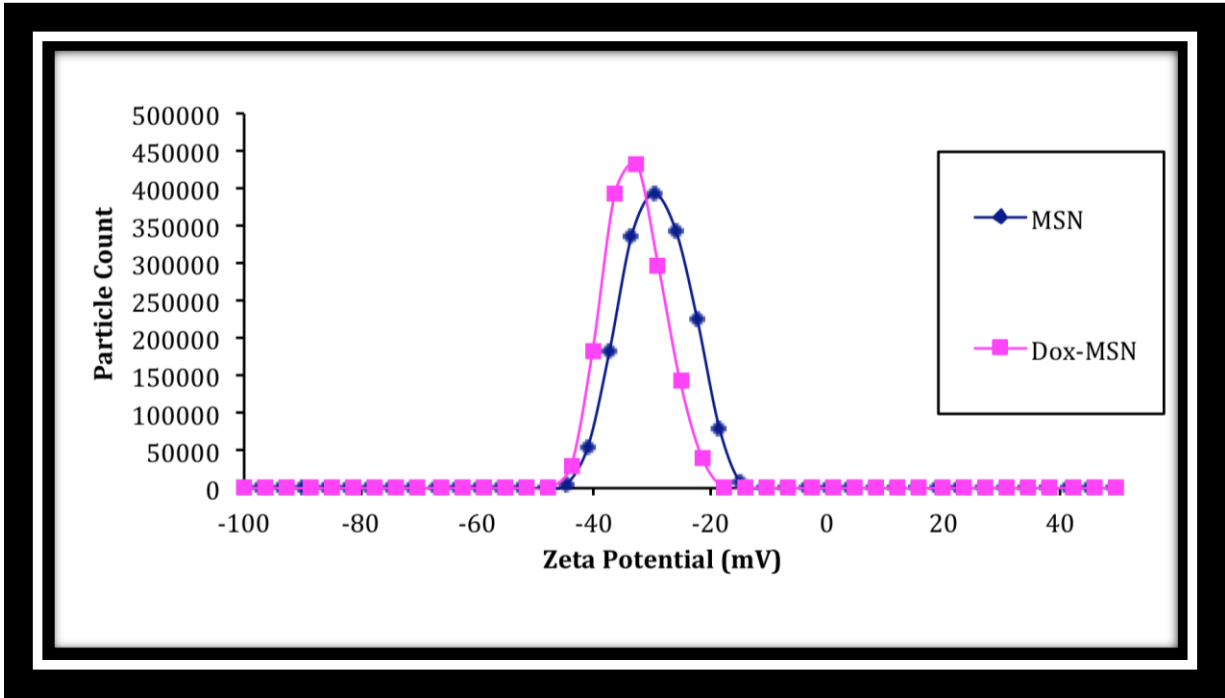
FIGURE 24: ZETA POTENTIAL RESULTS OF DOX BINDING TO MSN-6

Figure 24 shows the difference in zeta potential for MSN-6 (TEOS/APTS/PO4) and MSN-6 bound to Dox. There is a shift to the left when Dox is bound indicating that the sample has become more negative with the addition of the anionic nano drug particle.
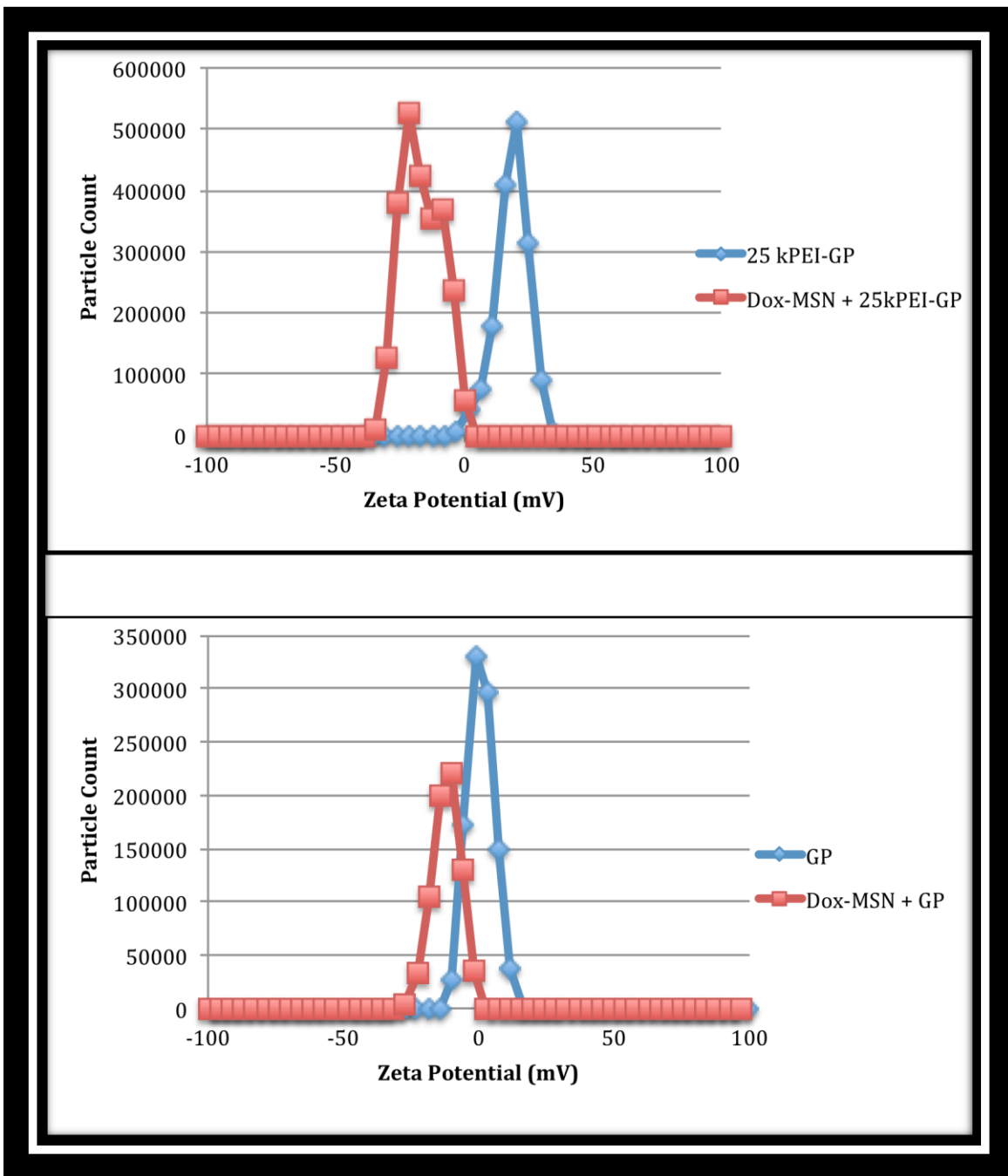
FIGURE 25: ZETA POTENTIAL OF DOX-MSN BOUND WITH 25K PEI-GP (TOP) AND GP (BOTTOM)

Figure 25 shows two sets of data for the zeta potential of the GP and GP-MSN-Dox complex. The upper figure shows the complex where the GP has been functionalized

while the lower figure shows the GP with no functionalization. There is a larger shift in the upper figure indicating that more MSN- Dox was bound.
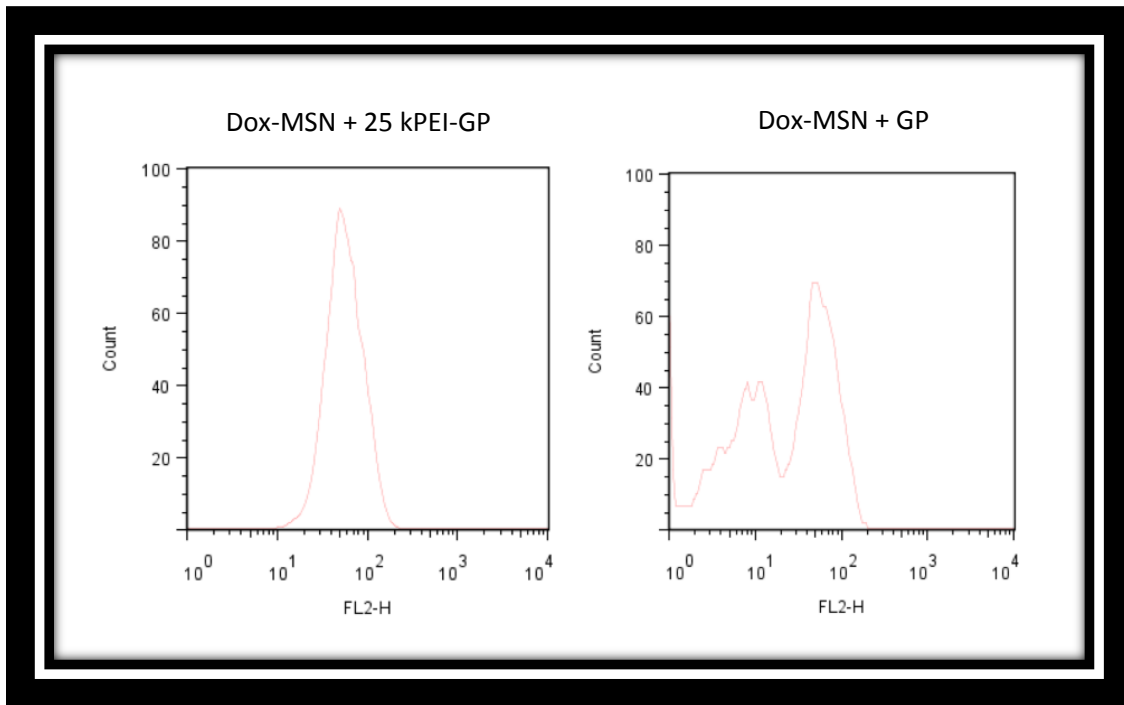
FIGURE 26: FACS RESULTS SHOWING SELECTIVE BINDING OF DOX-MSN TO 25 K PEI-GP

Figure 26 shows the results of FACS assay. These figures indicate the selective binding of Dox-MSN to the functionalized GP sample.
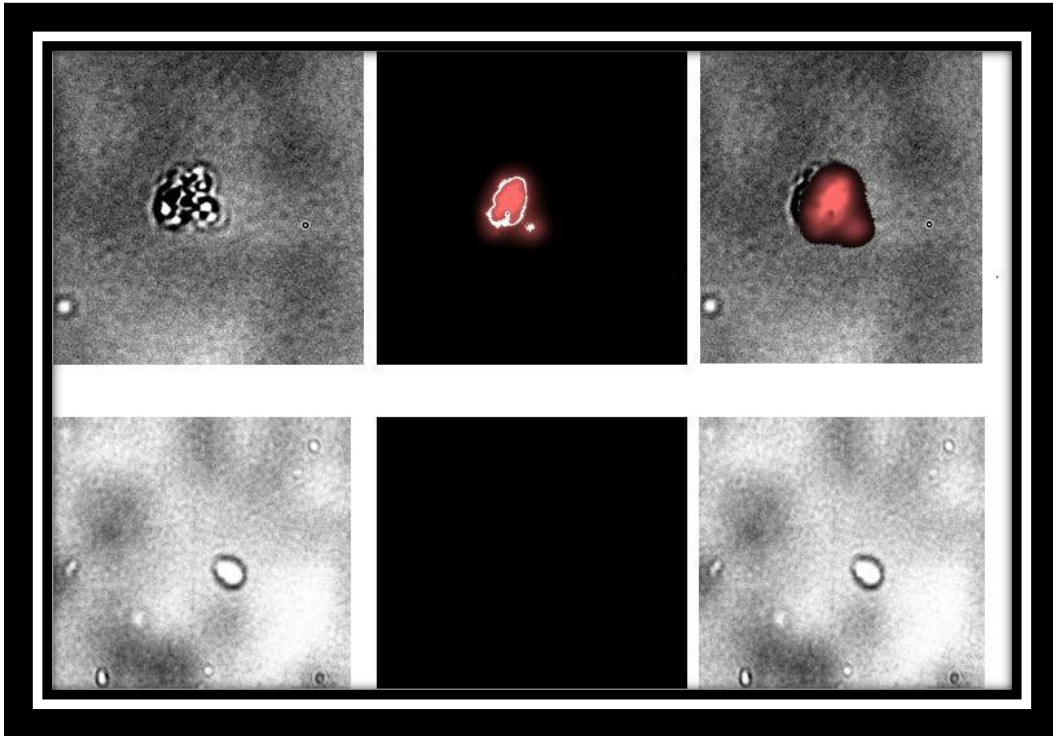
FIGURE 27: FLUORESCENT MICROSCOPY IMAGES SHOWING BINDING OF DOX-MSN TO 25 KPEI-GP (TOP) AND TO GP (BOTTOM)

Figure 27 shows microscopic images showing the binding of Dox-MSN to the functionalized GP (top) and the non-functionalized GP (bottom). Binding is only seen in the upper functionalized sample, showing the increased binding affinity with the PEI functionalization.

3 Hours: Dox-MSN-25 k PEI-GP
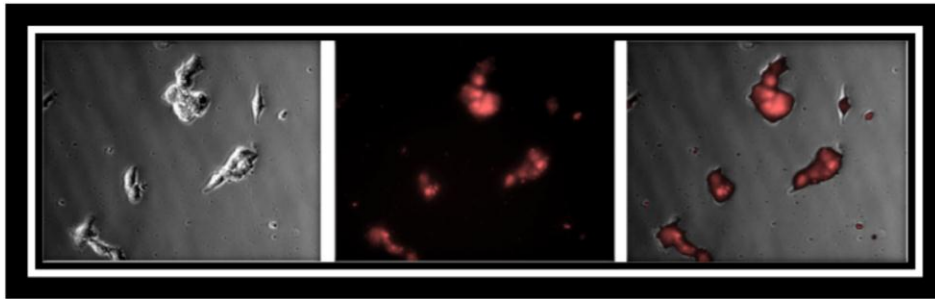
3 Hours: Dox-MSN
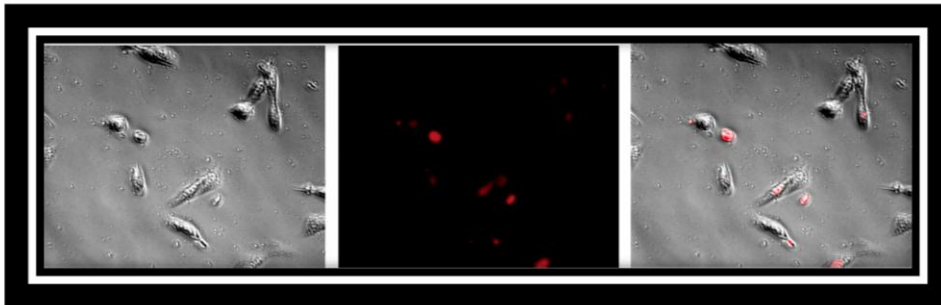
24 Hours: Dox-MSN 25k PEI-GP
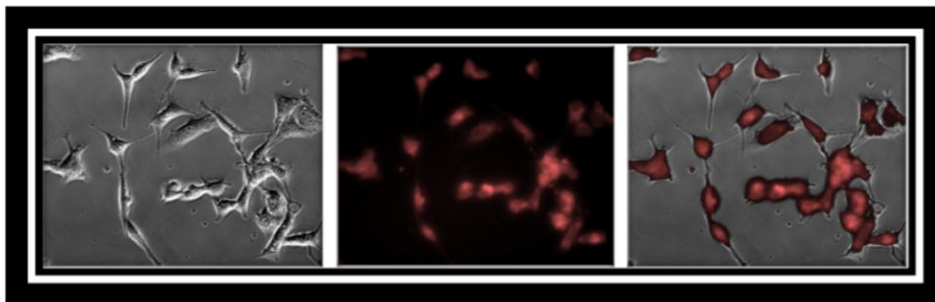
24 Hours: Dox-MSN

FIGURE 28: 20X FLUORESCENT MICROSCOPIC IMAGES SHOWING GLUCAN PARTICLE MEDIATED DOX DELIVERY INTO 3T3-D1 CELLS

Figure 28 shows the glucan particle mediated Dox delivery into 3T3-D1 cells. Indicating that the GP-25k PEI is more efficient in drug delivery due to this functionalization.
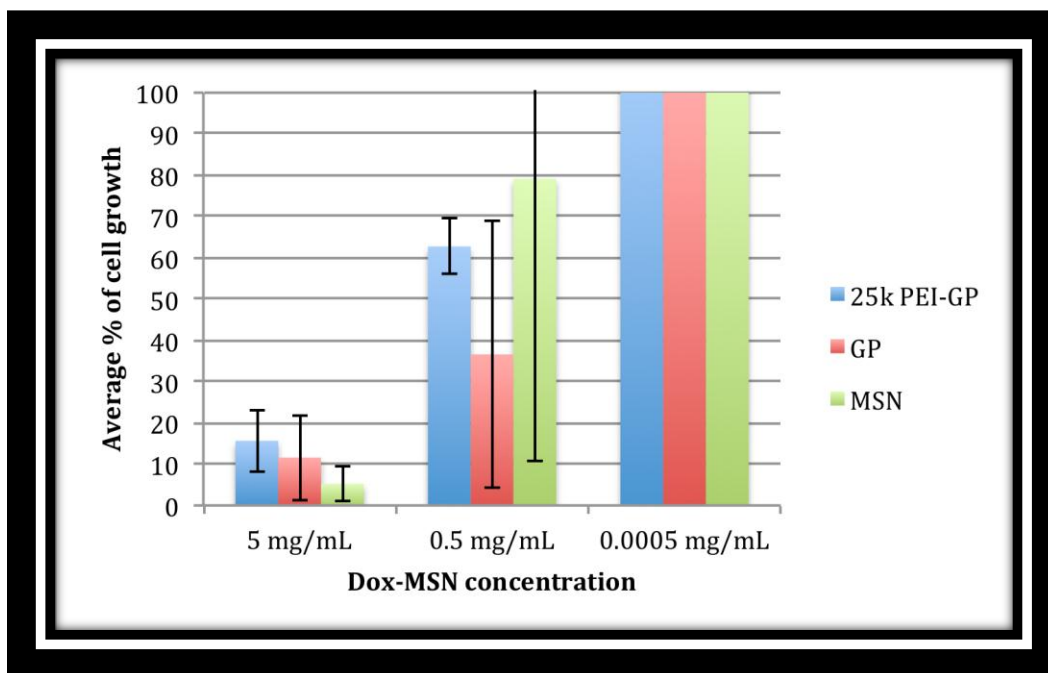
FIGURE 29: AVERAGE CELL GROWTH OF DIFFERENT DOX-MSN CONCENTRATIONS IN SUPERNATANT

Figure 29 shows the cell growth in the supernatant when different concentrations of Dox-MSN are applied. Higher concentrations showed lower levels of cell growth.
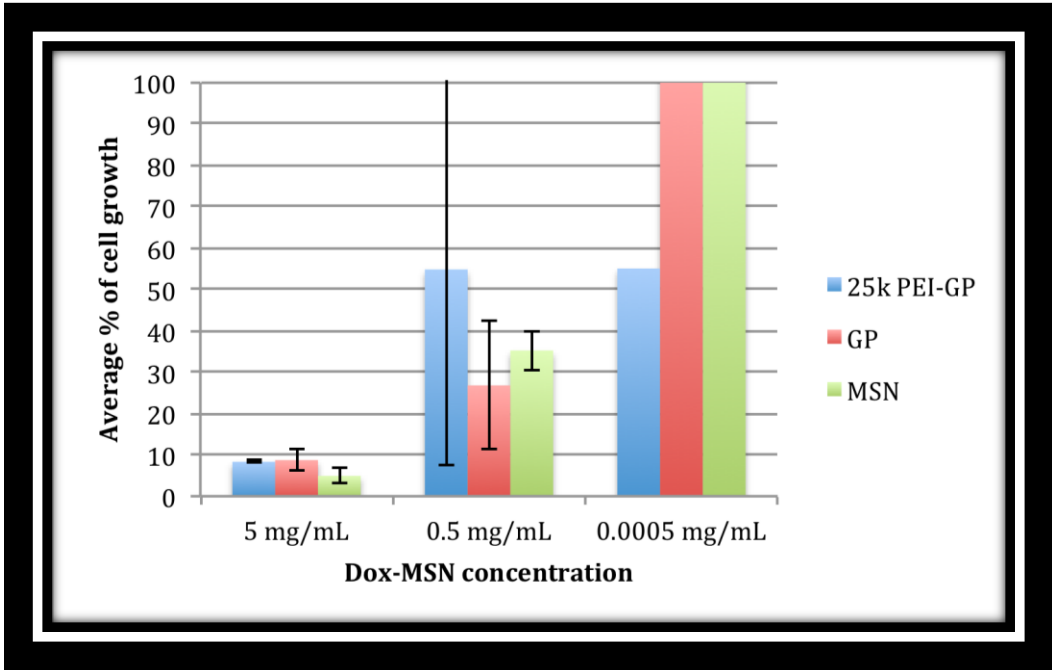
FIGURE 30: AVERAGE PERCENT OF CELL GROWTH OF DIFFERENT DOX-MSN
CONCENTRATIONS AFTER 3 HOURS.

Figure 30 shows the cell growth when different concentrations of Dox are applied

after 3 hours. The 25k PEI-GP-MSN drug complex showed the most cell growth

inhibition, at the lowest concentration.
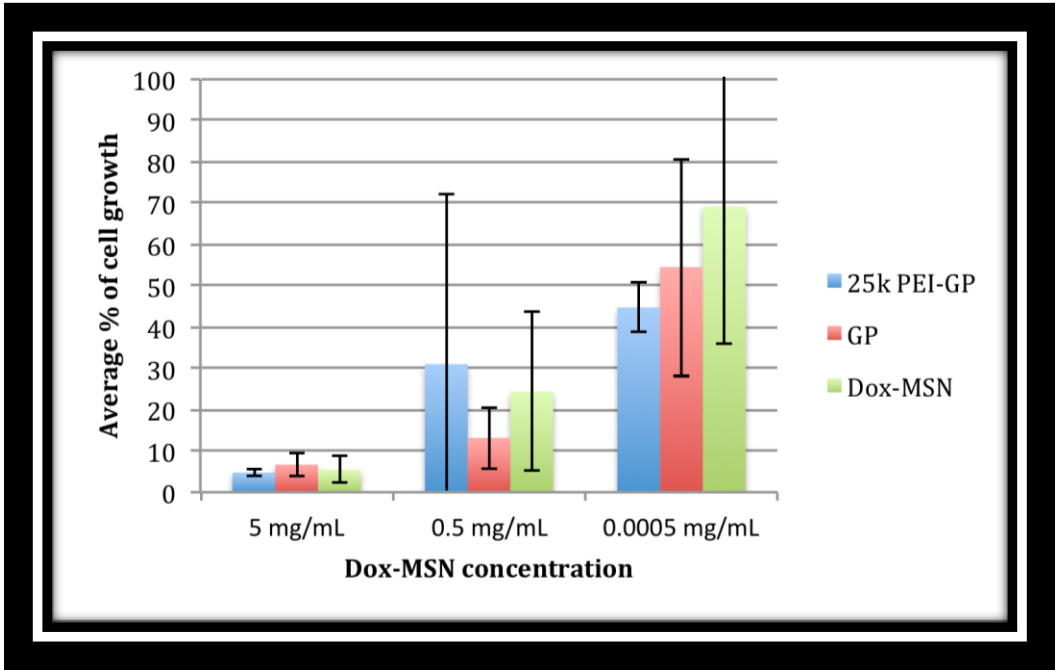
FIGURE 31: AVERAGE PERCENT OF CELL GROWTH OF DIFFERENT DOX-MSN CONCENTRATIONS AFTER 24 HOURS.

Figure 31 shows the cell growth when different concentrations of Dox are applied after 24 hours. Results again indicate that the 25k PEI-GP-MSN drug complex showed cell growth inhibition at the lowest drug concentration.
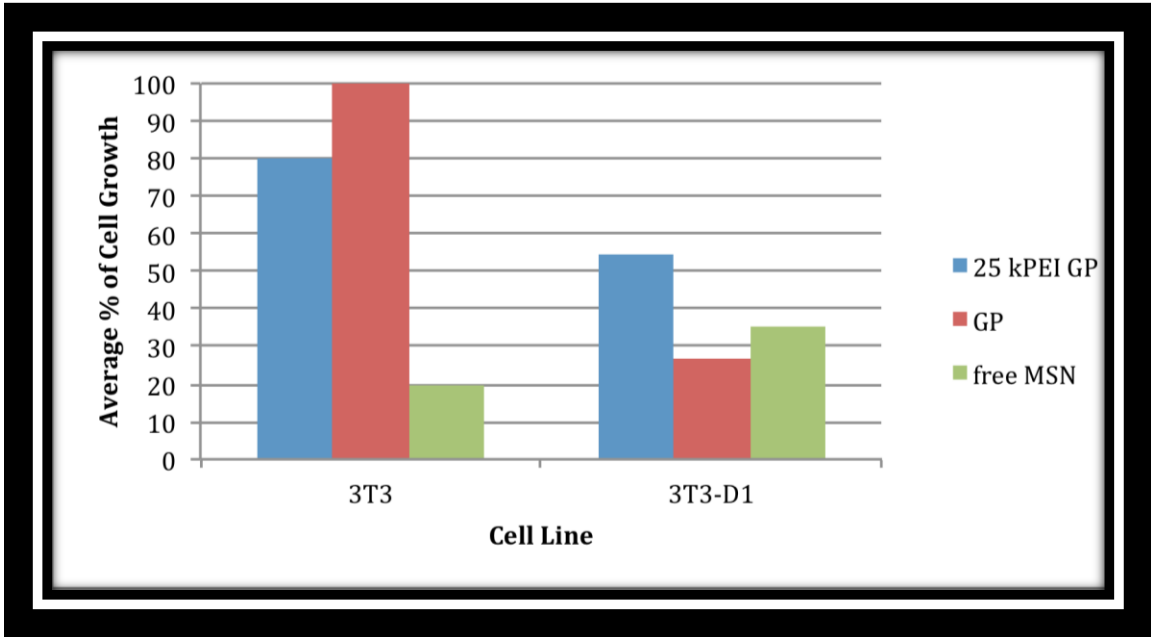
FIGURE 32: AVERAGE PERCENTAGE OF CELL GROWTH OF DOX-MSN AT A CONCENTRATION OF 0.5 MG DOX-MSN/ML

Figure 32 shows the average cell growth, data is presented for 3T3 cells with and without the glucan receptor (D1). The data presented showed higher growth inhibition in cells containing the glucan receptor.
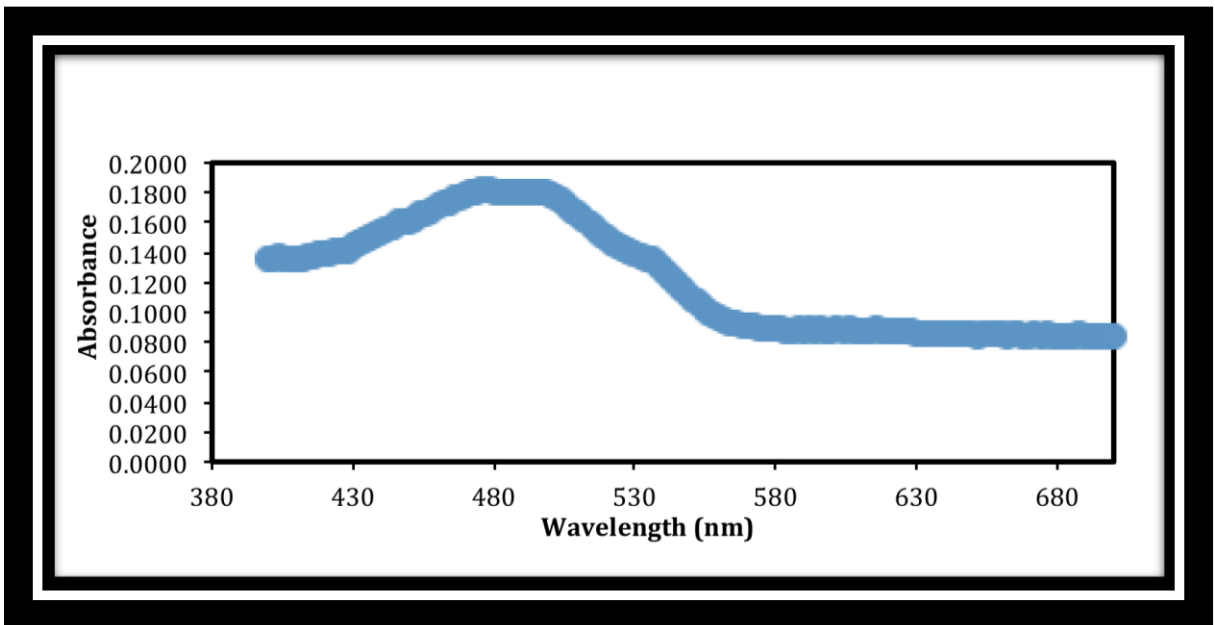
FIGURE 33: DOX EXCITATION SPECTRUM
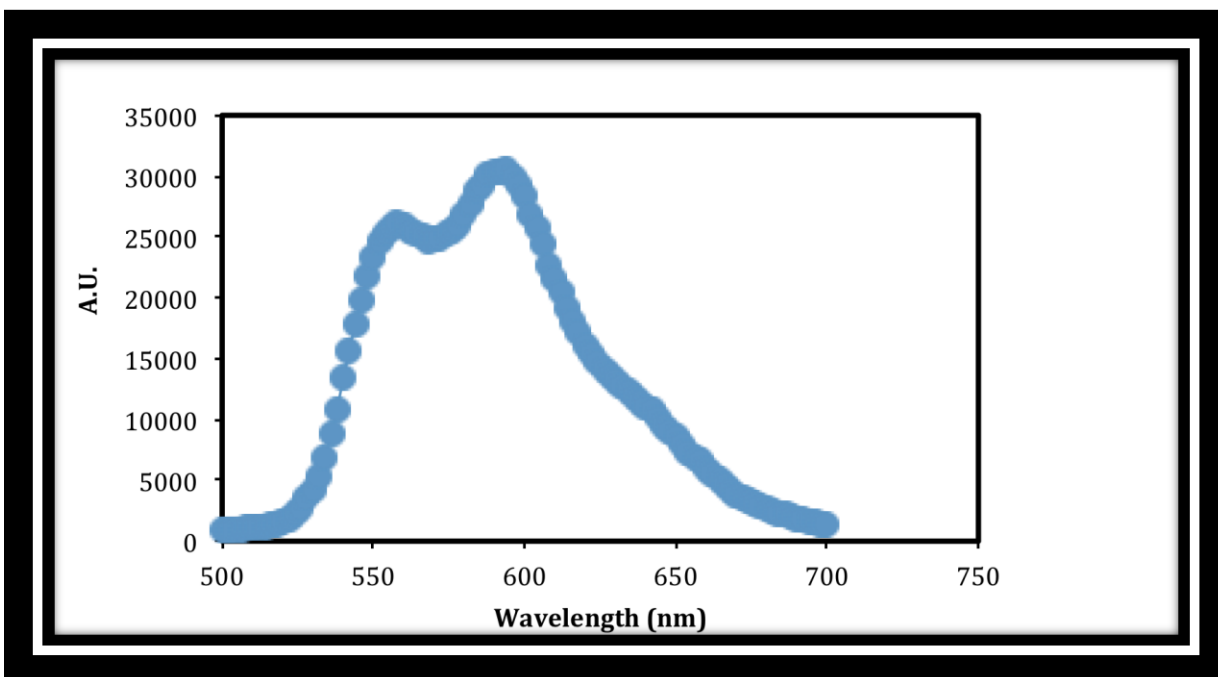
FIGURE 34: DOX EMISSION SPECTRUM

These figures show the Doxorubicin excitation/emission fluorescence spectra. The emission and excitation spectrum of Dox, as shown in figures 33 and 34, was measured to verify that the purchased compound was pure.
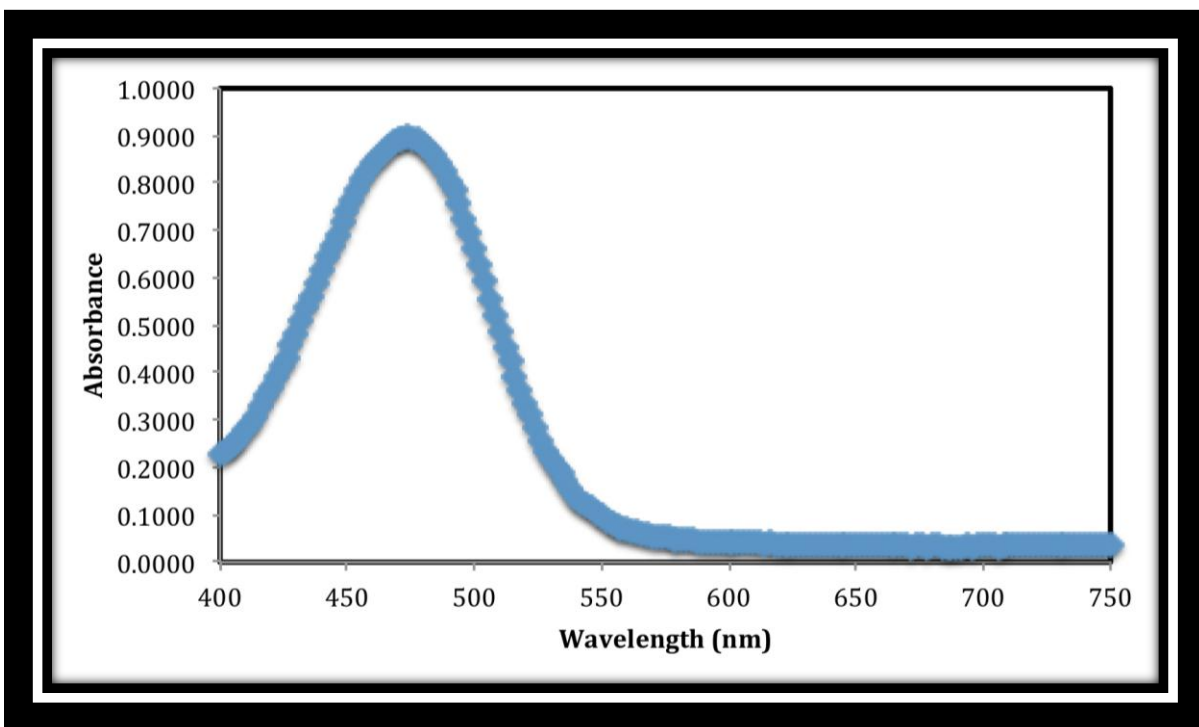
FIGURE 35: ABSORBANCE SPECTRUM OF RIF IN WATER

Figure 35 shows the visible absorption spectrum of rifampicin. This was completed to ensure that the sample was pure.